Nonhuman Primate Testing of the Impact of Different Regulatory T Cell Depletion Strategies on Reactivation and Clearance of Latent Simian Immunodeficiency Virus

Ranjit Sivanandham,[a,b] Adam J. Kleinman,[a] Paola Sette,[a,b] Egidio Brocca-Cofano,[b] Sindhuja Murali Kilapandal Venkatraman,[a,b] Benjamin B. Policicchio,[c] Tianyu He,[b] Cuiling Xu,[a,b] Julia Swarthout,[a,b] Zhirui Wang,[d] Ivona Pandrea,[b,c] Cristian Apetrei[a,c]

aDivision of Infectious Diseases, Department of Medicine, School of Medicine, University of Pittsburgh, Pittsburgh, Pennsylvania, USA
bDepartment of Pathology, School of Medicine, University of Pittsburgh, Pittsburgh, Pennsylvania, USA
cDepartment of Infectious Diseases and Microbiology, Graduate School of Public Health, University of Pittsburgh, Pittsburgh, Pennsylvania, USA
dDepartment of Surgery, School of Medicine, University of Colorado, Aurora, Colorado, USA

ABSTRACT Regulatory T cells (Tregs) may be key contributors to the HIV/SIV latent reservoir, since they harbor high levels of HIV/SIV; reverse CD4+ T cell immune activation status, increasing the pool of resting CD4+ T cells; and impair CD8+ T cell function, favoring HIV persistence. We tested the hypothesis that Treg depletion is a valid intervention toward an HIV cure by depleted Tregs in 14 rhesus macaque (RM) controllers infected with SIVsab, the virus that naturally infects sabaeus monkeys, through different strategies: administration of an anti-CCR4 immunotoxin, two doses of an anti-CD25 immunotoxin (interleukin-2 with diphtheria toxin [IL-2-DT]), or two combinations of both. All of these treatments resulted in significant depletion of the circulating Tregs (>70%) and their partial depletion in the gut (25%) and lymph nodes (>50%). The fractions of CD4+ T cells expressing K_i-67 increased up to 80% in experiments containing IL-2-DT and only 30% in anti-CCR4-treated RMs, paralleled by increases in the inflammatory cytokines. In the absence of ART, plasma virus rebounded to 10^3 vRNA copies/ml by day 10 after IL-2-DT administration. A large but transient boost of the SIV-specific CD8+ T cell responses occurred in IL-2-DT-treated RMs. Such increases were minimal in the RMs receiving anti-CCR4-based regimens. Five RMs received IL-2-DT on ART, but treatment was discontinued because of high toxicity and lymphopenia. As such, while all treatments depleted a significant proportion of Tregs, the side effects in the presence of ART prevent their clinical use and call for different Treg depletion approaches. Thus, based on our data, Treg targeting as a strategy for HIV cure cannot be discarded.

IMPORTANCE Regulatory T cells (Tregs) can decisively contribute to the establishment and persistence of the HIV reservoir, since they harbor high levels of HIV/SIV, increase the pool of resting CD4+ T cells by reversing their immune activation status, and impair CD8+ T cell function, favoring HIV persistence. We tested multiple Treg depletion strategies and showed that all of them are at least partially successful in depleting Tregs. As such, Treg depletion appears to be a valid intervention toward an HIV cure, reducing the size of the reservoir, reactivating the virus, and boosting cell-mediated immune responses. Yet, when Treg depletion was attempted in ART-suppressed animals, the treatment had to be discontinued due to high toxicity and lymphopenia. Therefore, while Treg targeting as a strategy for HIV cure cannot be discarded, the methodology for Treg depletion has to be revisited.

The difficulty in curing HIV infection stems from the virus ability to persist in long-term reservoirs and our incapacity to identify and eliminate these cells (1, 2). An HIV-infected cell can lay dormant for many years (3–5). Antiretroviral therapy (ART) successfully suppresses replicative virus and thus controls the deleterious consequences of the active virus replication but does not eliminate the latent reservoirs (3–6). The interest for HIV cure research was prompted by the Berlin patient, the first case of cured HIV infection (7, 8) and, more recently, by the second confirmed cured case, the London patient (9). Both received bone marrow transplants from donors with a CCR5-Δ32 mutation (7–9). Due to the dangerous nature of this treatment and the limited availability of donors carrying this mutation, the approach is not scalable as a universal cure strategy. Therefore, the HIV field is actively searching for more tolerable strategies toward an HIV cure.

Of the many tested cure strategies, the "shock and kill" is one of the most studied. In this approach, the latently infected cells are "shocked" with latency reversal agents (LRAs) to induce expression of latent proviruses, with the cells in which virus expression is induced being eliminated by viral cytopathic effects or host immune responses (10). *De novo* infection of susceptible cells by the LRA-induced virus is prevented by ongoing ART (11, 12). While the rationale of this approach appears reasonable, the results to date have not fulfilled expectations. Thus, the vast majority of LRAs did not lead to potent and extensive induction of latent proviruses (13, 14), with only very small fractions of proviruses present in resting $CD4^+$ T cells being reactivated by a single round of LRA administration (15, 16). Only recently promising reactivation data were reported (17). Even more daunting was the observation that LRA administration did not result in viral cytopathic effect-mediated cell death (12), and thus elimination of the reactivated resting $CD4^+$ T cells in which expression of latent proviruses was induced was proven more challenging than originally believed (18). In immunosuppressed patients, even in those virally suppressed with ART, HIV-specific cytotoxic T lymphocytes (CTLs) are functionally impaired (19), with viral clearance by CTLs only occurring in elite controllers (20). Meanwhile, some LRAs, such as the histone deacetylase inhibitors were reported to impair CTL functions (21). Finally, much of the virus present in latently infected cells in individuals that started ART in the chronic phase of infection contains escape mutations for immunodominant epitopes (22) or is defective and cannot be reactivated (23). As such, the "shock and kill" approaches are currently questioned in their ability to ostensibly reduce the latent reservoir (24, 25), and a general consensus emerged that new strategies to improve both shock and kill components are needed in order to improve HIV reservoir purging.

We have previously suggested that targeting regulatory T cells (Tregs), an immune subset of T cells with specific function (26), which are enriched in the lymph nodes (LNs) and gastrointestinal (GI) mucosa, may play a central role in shaping the HIV reservoir and improving HIV/SIV-specific immune responses (27). As such, Treg depletion might be an effective strategy toward a cure. In HIV/SIV infection, the frequency of circulating Tregs directly correlates with viral loads (VLs) and disease progression and inversely correlates with SIV-specific cytotoxic T lymphocyte responses in circulation and lymphoid tissue (28–33). Tregs themselves can be infected by HIV/SIV (33–35) and contain higher levels of HIV/SIV DNA than non-Tregs, suggesting that they may represent a nonnegligible fraction of the viral reservoir (34, 36). Furthermore, Tregs have a better survival from SIV/HIV infection (34) than non-Tregs, a characteristic that could also contribute to Tregs being a key persistent HIV reservoir. Through their regulatory function, Tregs also have the potential to significantly shape the viral reservoir. Thus, during the acute HIV/SIV infection, Tregs may decisively contribute to the rapid reservoir seeding, by reversing the activation status of $CD4^+$ T cells (33, 37–40), thereby pushing them into latency. During chronic HIV/SIV infection, multiple lines of evidence support Treg suppression of protective effector immune responses: (i) Treg expansion correlates with loss of CTL function (40–42); (ii) *Ex vivo* Treg depletion from blood and LNs enhances T cell responses to HIV/SIV antigens (43); (iii) higher perforin/transcriptional factor forkhead box 3 (FoxP3) ratios are associated with the nonprogressor status;

and (iv) HLAB27$^+$and B57$^+$ HIV-specific CD8$^+$ T cells from controllers evade Tregs (31, 44). This Treg suppression of virus-specific immune responses may impact the efficacy of the "shock and kill" strategies, which require effective killing of the reactivated virus.

Altogether, these findings strongly suggest that Tregs may be a critical cellular subset that shapes the formation, persistence, and reactivation of the viral reservoir (45). Their depletion may impact the reservoir either directly, through reduction of one of its components, or indirectly, by significantly altering SIV-specific immune responses. Therefore, we proposed Treg depletion as a novel HIV cure strategy with a 3-fold benefit: (i) direct reduction of the latent reservoir, (ii) arresting driving activated infected cells into latency, and (iii) improving the suppressive capacities of the SIV-specific T cells (27).

Treg depletion *in vivo* is complicated by the fact that Tregs do not express a specific surface marker. FoxP3, which is currently the best Treg marker, is intracellular (46–48) and cannot be targeted without altering the cell membrane. Therefore, Treg depletion strategies rely on targeting surface surrogate markers expressed by Treg subsets: CD25 (denileukin diftitox; Daclizumab), CCR4 (anti-CCR4-DT, Mogamulizumab), or CTLA-4 (Ipilimumab). As such, none of the current Treg depletion strategies can induce full Treg depletion (27, 49–52). Note, however, that post-depletion persistence of residual Tregs is not necessarily daunting, since even a partial Treg depletion alters their regulatory capacities (27, 49–52), while preventing the massive autoimmune and inflammatory reactions associated with their complete absence, as reported to occur in human newborns without functional Tregs (53, 54) or in mice with Treg ablation (55, 56).

Of the Treg depletion strategies, we employed two and targeted either CD25 or CCR4. CD25 is essential for Treg differentiation (57) and can be targeted with interleukin-2 (IL-2), which exhibits its biological activity by binding to CD25 on the cell surface (58). We previously showed that administration of a commercially available IL-2 immunotoxin, denileukin diftitox (Ontak), a fusion protein in which the IL-2 segment is fused to the enzymatically active and membrane translocation domain of diphtheria toxin, can induce Treg depletion in two nonhuman primate (NHP) species (27, 49). In a model of SIV controlled infection of rhesus macaques (RMs), Ontak administration induced effective plasma viral reactivation and boosted SIV-specific T cell responses, suggesting that Treg depletion could indeed represent a viable HIV cure strategy (27). Since Ontak has been discontinued due to problems with the protein purification, we evaluated here a new IL-2-diphtheria toxin (IL-2-DT) immunotoxin produced with a different purification system (59).

The second strategy was based on the use of immunotoxin that targeted CCR4. CCR4 is a receptor for CCL17/CCL22, which is expressed with high frequency on the surface of a subset of Tregs (60) and can be targeted with an anti-CCR4 antibody.

We thus tested these two immunotoxins individually and, to improve the efficacy of Treg depletion, we also tested their combinations and assessed their impact on SIV reactivation and residual reservoir. We report that the use of these novel immunotoxins effectively but transiently led to Treg depletion from circulation, LNs, and at mucosal sites, which subsequently leads to an increase in SIV-specific CD4$^+$ and CD8$^+$ T cells, including those with a lytic phenotype (CD107a). Treg-depleting agents had minimal toxicity when administered to SIV-infected, ART-naive RMs. All Treg depletion strategies induced massive increases of systemic immune activation, yet only the IL-2-DT administration resulted in detectable viral reactivation. However, we also report that IL-2-DT administration to SIV-infected RMs on ART causes dangerous toxicity and severe lymphopenia, including the reduction of the SIV-specific T cells. As such, we report that, while the current immunotoxins tested cannot be used as HIV cure agents due to severe toxicities when associated with ART, Treg depletion could be combined with other more potent LRAs to boost SIV-specific immune responses and improve HIV reactivation from the latent reservoir.
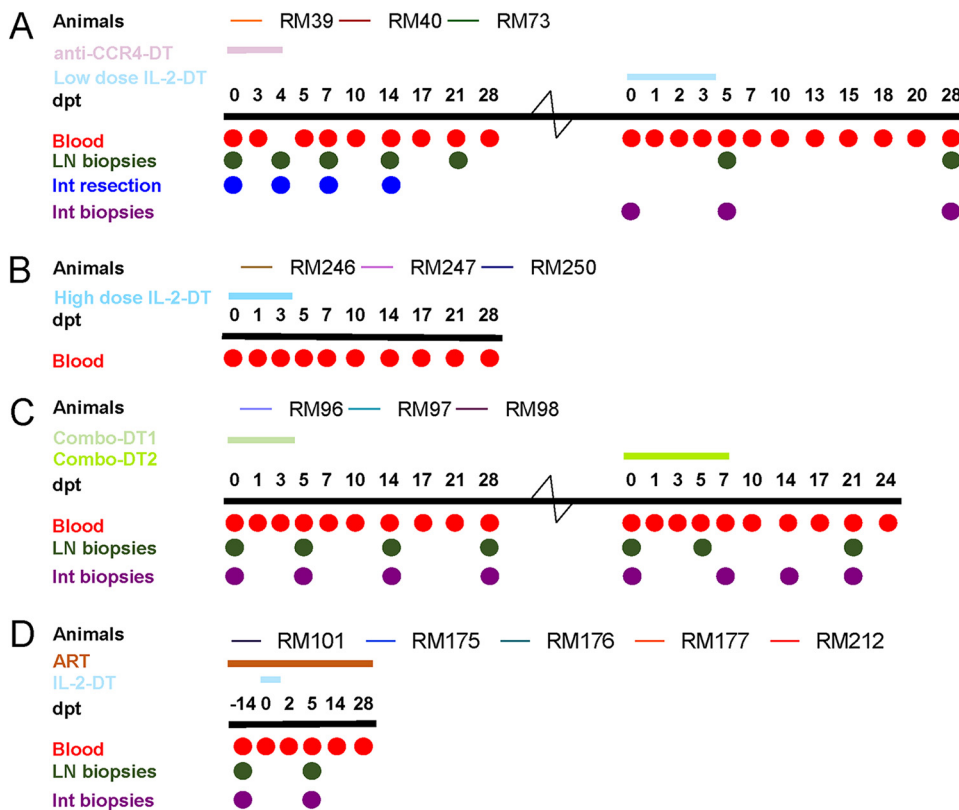
FIG 1 Experimental design of the study. Fourteen rhesus macaques (RMs) were infected i.v. with 300 TCID$_{50}$ SIVsab92018, and they were allowed to robustly control virus replication. Then, after >1 year of viral control, three RMs received anti-CCR4-diphtheria toxin (DT) and low-dose IL-2-DT (A), three RMs received a high-dose IL-2-DT (B), and three RMs received combinations of anti-CCR4-DT and IL-2-DT in a ratio of 1.62:1 by weight (Combo-DT1) and in a ratio of 1:1.62 (Combo-DT2) (C). Finally, five RM controllers received 14 days of antiretroviral therapy (ART), followed by the administration of the low-dose IL-2-DT on ART (D). After each treatment, the animals were monitored for an average of 28 days posttreatment (dpt). Treg-depleting immunotoxin administrations are illustrated as color-coded lines over each study group. Blood, lymph node (LN), and duodenal biopsy specimens were collected at numerous experimental points, as indicated by the circles.

RESULTS

Study design. Fourteen SIVsab-infected RM controllers (61, 62) were used to assess the impact of Treg depletion on SIV reactivation (Fig. 1). Five treatment conditions for Treg depletion and SIV reactivation were tested, which included different doses and/or combinations of an IL-2 diphtheria toxin (IL-2-DT), an anti-CCR4 diphtheria toxin (anti-CCR4-DT), and the combination of these.

The first group of three SIVsab-infected RM controllers received anti-CCR4-DT which was administered intravenously (i.v.), at a dose of 25 μg/kg, twice a day (BID) for 5 days. These RMs were monitored for up to 28 days posttreatment (dpt) initiation. Blood and superficial LN biopsy specimens were serially collected, and intestinal resections were performed pretreatment in all the animals and then at different posttreatment time points for each animal. The RMs were then rested for enough time to allow the immune system to stabilize, followed by administration of 25 μg/kg of IL-2-DT (low-dose IL-2-DT), i.v., BID for 5 days, with a 28-dpt follow-up and a thorough collection of blood, LNs, and intestinal biopsy specimens.

The second group of three SIVsab-infected RM controllers received 35 μg/kg of IL-2-DT (high-dose IL-2-DT), i.v., BID for 5 days and were monitored for up to 28 dpt. Blood was collected at key time points.

The third group of three SIVsab-infected RM controllers received a combination of anti-CCR4-DT and IL-2-DT, in a ratio of 1.62:1 by weight (Combo-DT1), which was calculated based on the molecular weight of the compounds, and administered as a

total of 25 μg/kg, i.v., BID for 5 days. One animal was lost during follow-up due to clinical deterioration. In the remaining two RMs, we reversed the ratio of the anti-CCR4-DT and IL-2-DT drug combination to 1:1.62 (Combo-DT2) and tried a different dosing regimen of 50 μg/kg, i.v., BID on the first day, and 25 μg/kg, i.v., BID for 6 days, since another study showed that a similar treatment schedule achieved a better Treg depletion (63). Blood, superficial LN biopsy specimens, and intestinal biopsy specimens were collected for both treatments.

Finally, a fourth group of five SIVsab-infected RM controllers were used to assess the impact of Treg depletion on SIV-infected RMs on ART. The RMs were infected with SIVsab, allowed to spontaneously control viral replication to undetectable levels for >1 year, and then they received an ART coformulation of Tenofovir disoproxil fumarate (TDF), emtricitabine (FTC), and dolutegravir (DTG) (64) for 14 days, followed by the administration of 25 μg/kg of IL-2-DT, i.v., BID. However, after the administration of only 3 IL-2-DT doses, the treatment had to be stopped due to severe clinical discomfort.

Treg depletion. Tregs are difficult to define, as there is no single marker to identify them (45). The most specific marker for Tregs is currently FoxP3 (46–48), and, as such, unless otherwise specified, throughout this study we will refer to Tregs as to FoxP3^{high} CD4$^+$ T cells.

All individual immunotoxin treatments, i.e., anti-CCR4-DT, low-dose IL-2-DT, and high-dose IL-2-DT, achieved depletion of >70% of circulating Tregs (Fig. 2A). Depletion was statistically significant with both IL-2-DT regimens. Circulating FoxP3^{high} CD8$^+$ T cells were also similarly depleted, with statistical significance achieved in both IL-2-DT regimens (Fig. 2B). Interestingly, both the FoxP3^{high} CD4$^+$ T cells and the FoxP3^{high} CD8$^+$ T cells rebounded immediately after treatment cessation (peaking between 10 and 14 dpt) and reached pretreatment levels at around 21 to 28 dpt. This transient Treg boost was likely due to the generalized immune activation seen after Treg-depleting treatment administration.

Similarly, more than 42 to 58% of Tregs were depleted in the superficial LNs with both IL-2-DT regimens (Fig. 2C), which, however, did not reach statistical significance.

In the gut, minimal to no Treg depletion occurred after anti-CCR4-DT administration (Fig. 2D), while a discernible Treg depletion was observed following low-dose IL-2-DT administration (Fig. 2D). Similar to the LNs, Treg depletion in the gut did not reach statistical significance after either of these treatments.

Impact on other T cell populations. Total CD4$^+$ T cell counts were moderately, but significantly, reduced after each treatment, followed by a rapid rebound by 10 to 14 dpt and stabilization to pretreatment levels by 21 to 28 dpt (Fig. 2E). Similarly, CD8$^+$ T cell counts were impacted by the Treg-depleting treatments. However, large increases in the CD8$^+$ T cell counts occurred after the high-dose IL-2-DT administration ($P = 0.0018$) (Fig. 2F).

Postdepletion Treg activation. CD39 and CD73 are ectonucleases which generate extracellular adenosine, are essential for Treg immunoregulatory capacity (65), and are therefore used as markers of Treg activation (66). We thus assessed the Treg fraction expressing CD39 or CD73. Minimal change in CD39 and CD73 expressions occurred with anti-CCR4-DT (Fig. 3A and B). A minimal transient boost was observed after the low-dose IL-2-DT treatment, which was statistically significant ($P = 0.0276$ and $P = 0.0640$ for CD39 and CD73, respectively) (Fig. 3A and B). Conversely, with the high-dose IL-2-DT there was a large and statistically significant increase in the expression of both markers by the Tregs ($P = 0.0125$ and $P = 0.0042$ for CD39 and CD73, respectively), which peaked 5 dpt and returned to normal by 10 dpt (Fig. 3A and B).

T cell immune activation and inflammation. The levels of circulating T cell immune activation were assessed by measuring the fraction of T cells expressing the proliferation marker K_i-67. Each of the Treg-depleting immunotoxins induced a dramatic increase in the T cell fraction expressing K_i-67, which peaked between 10 and 14 dpt, reaching levels representing up to 50 to 80% of circulating CD4$^+$ T cells (Fig. 3C) and 60–90% of circulating CD8$^+$ T cells (Fig. 3D). The increase in K_i-67 expression on
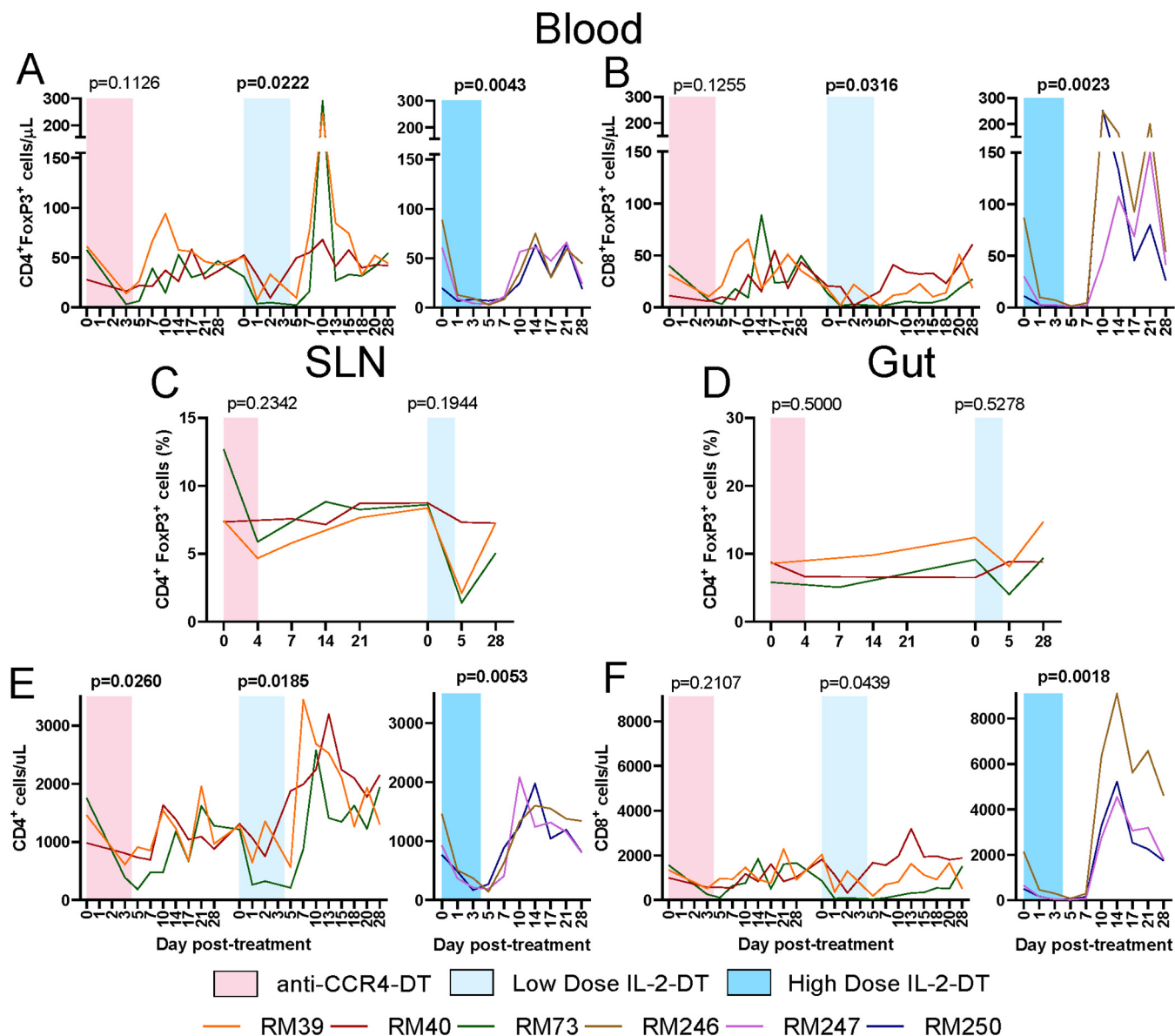
Blood

FIG 2 (A to D) Efficacy of the FoxP3high CD4+ T cell (A) and FoxP3high CD8+ T cell (B) depletion in circulation after treatments with anti-CCR4-diphtheria toxin (DT), low-dose IL-2-DT, and high-dose IL-2-DT, and FoxP3high CD4+ T cell depletion in superficial lymph nodes (LNs) (C) and in the intestine (D) with anti-CCR4-DT treatment and low-dose IL-2-DT. (E and F) The y axes illustrate the levels of FoxP3high cells. Changes in the circulating CD4+ T cell counts (E) and CD8+ T cell counts (F) following the administration of the anti-CCR4-DT, low-dose IL-2-DT, and high-dose IL-2-DT. The y axes illustrate the levels of CD4+ or CD8+ T cells/μl; the x axes illustrate the number of days post-DT administration. A Kruskal-Wallis test was performed for FoxP3high CD4+ T cell depletion in superficial LNs and in the intestine with anti-CCR4-DT treatment, and a Friedman test was performed for all other parameters for each treatment. $P < 0.05$ (boldface) values were considered significant. Different treatments are color-coded.

CD4+ T cells reached statistical significance after the administration of high-dose IL-2-DT ($P = 0.0026$), with trends being seen with the other treatments. Conversely, the increases in K_i-67 expression on CD8+ T cells reached significance after both IL-2-DT treatments ($P = 0.0104$ and $P = 0.0054$, respectively. The increases in K_i-67 expression by the circulating T cell subsets were minimal after the anti-CCR4-DT treatment (Fig. 3C and D).

In the superficial LNs, the fractions of the CD4+ and CD8+ T cells expressing K_i-67 increased following both anti-CCR4-DT and low-dose IL-2-DT administration, though at lower levels than those seen in blood, with statistical significance being reached only after anti-CCR4-DT ($P = 0.0204$ and $P = 0.0014$ for CD4+ and CD8+ T cells, respectively) (Fig. 4A and B). Only minimal increases of the K_i-67 expression by the T cells were
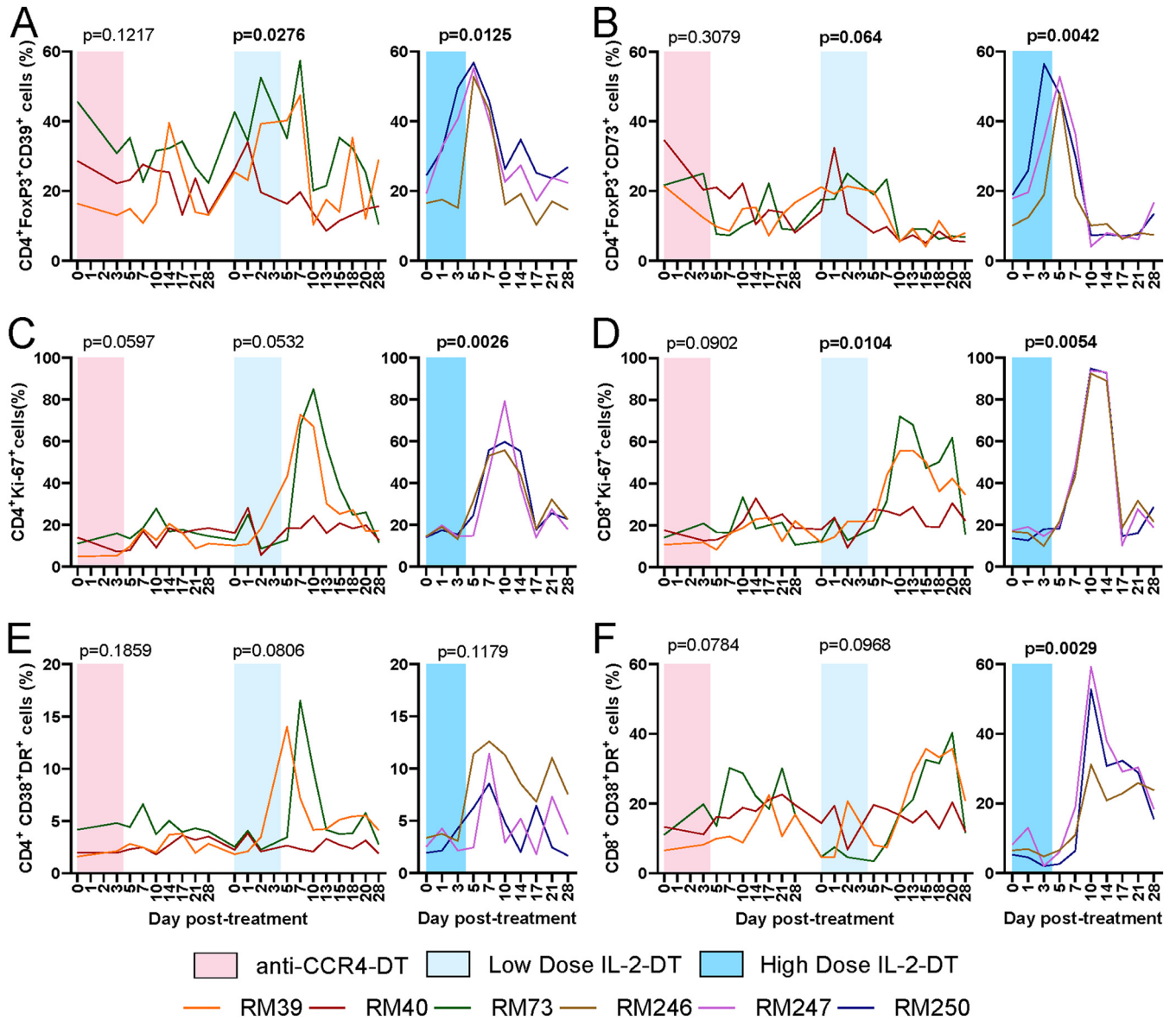
FIG 3 (A) Dynamics of the CD39$^+$ Tregs (FoxP3^{high} CD4$^+$ T cells) after the administration of anti-CCR4-DT, low-dose IL-2-DT, and high-dose IL-2-DT. (B) Dynamics of the CD73$^+$ Tregs after the administration of anti-CCR4-DT, low-dose IL-2-DT, and high-dose IL-2-DT. The y axes illustrate the frequency of CD39$^+$ or CD73$^+$ Tregs (%). (C and D) Dynamics of T cell immune activation, as illustrated by the levels of K_i-67 expression by the CD4$^+$ (C) and CD8$^+$ (D) T cells after administration of anti-CCR4-DT, low-dose IL-2-DT, and high-dose IL-2-DT. (E and F) Dynamics of T cell immune activation, as illustrated by the levels of CD38 and HLA-DR coexpression by the CD4$^+$ (E) and CD8$^+$ (F) T cells after administration of anti-CCR4-DT, low-dose IL-2-DT, and high-dose IL-2-DT. The y axes illustrate the frequency (%) of activated CD4$^+$ or CD8$^+$ T cells; the x axes illustrate the number of days post-DT administration. Different treatments are color-coded. A Friedman test was performed individually for each treatment, and $P < 0.05$ (boldface) values were considered significant.

observed after the administration of low-dose IL-2-DT (Fig. 4A and B); yet, one should note that these minimal increases might be the result of the sample collection schedule, with no LNs being collected between 6 and 27 dpt, which might have resulted in missing the peak of K_i-67 expression.

In the gut, K_i-67 expression on the T cells increased following both immunotoxins (Fig. 4E and F). However, these increases did not reach statistical significance.

We also assessed circulating T cell activation by measuring the T cell fraction expressing HLA-DR and CD38. On the CD4$^+$ T cells, HLA-DR and CD38 coexpression peaked between 5 and 10 dpt, albeit not reaching statistical significance, with trends being seen after the administration of the low-dose IL-2-DT (Fig. 3E). Meanwhile, the HLA-DR and CD38 coexpression on circulating CD8$^+$ T cells peaked later, between 10
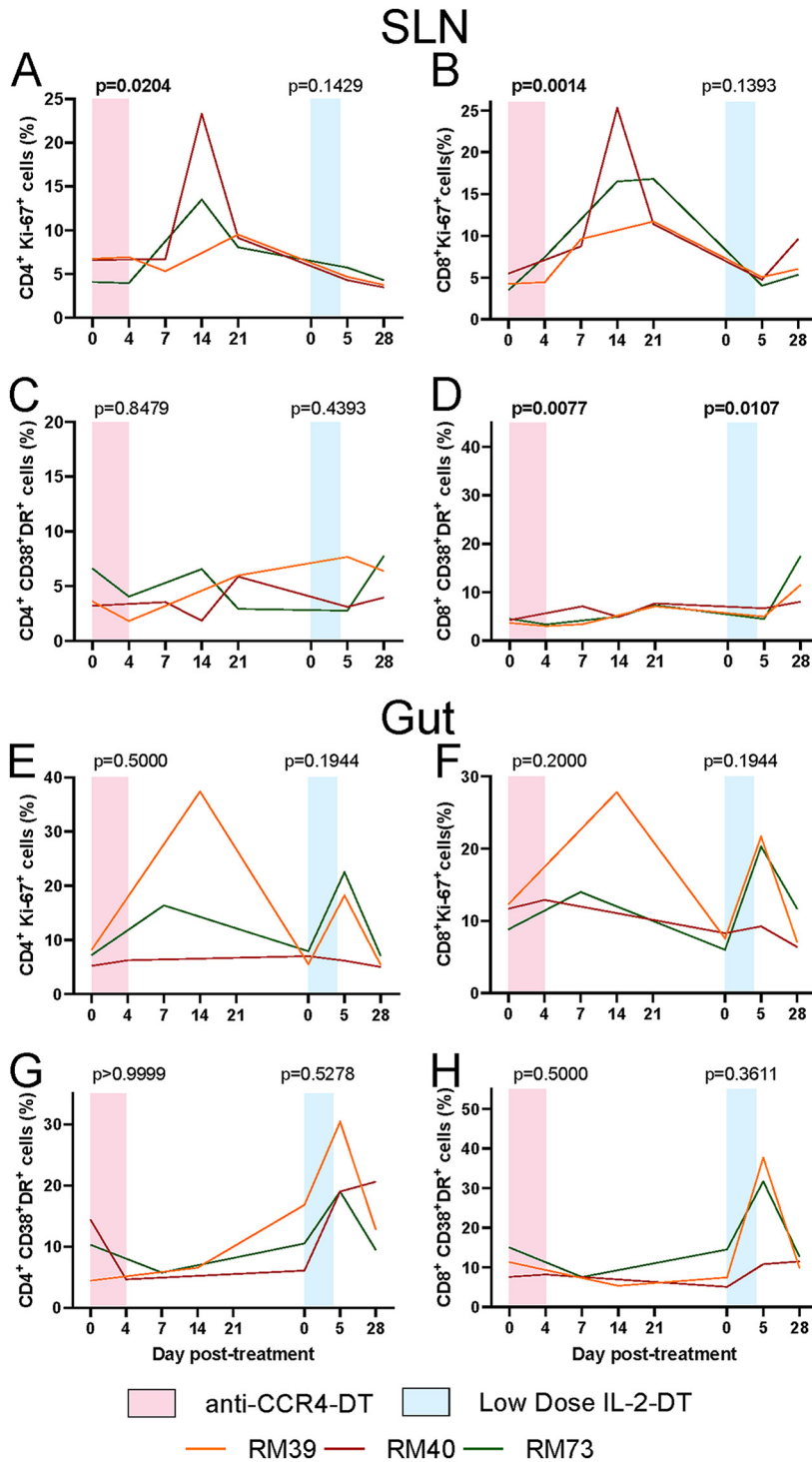
FIG 4 (A and B) Dynamics of T cell immune activation in the LNs, as illustrated by the levels of K_i-67 expression by the CD4+ (A) and CD8+ (B) T cells after administration of anti-CCR4-DT and low-dose IL-2-DT. (C and D) Dynamics of T cell immune activation in the LNs, as illustrated by the levels of CD38 and HLA-DR coexpression by the CD4+ (C) and CD8+ (D) T cells after administration of anti-CCR4-DT and low-dose IL-2-DT. (E and F) Dynamics of T cell immune activation in the intestine, as illustrated by the levels of K_i-67 expression by the CD4+ (E) and CD8+ (F) T cells after administration of anti-CCR4-DT and low-dose IL-2-DT. (G and H) Dynamics of T cell immune activation in the intestine, as illustrated by the levels of CD38 and HLA-DR coexpression by the CD4+ (G) and CD8+ (H) T cells after administration of anti-CCR4-DT and low-dose IL-2-DT. Different treatments are color-coded. The y axes illustrate the frequency (%) of activated CD4+ or CD8+ T cells; the x axes illustrate the number of days post-DT administration. A Kruskal-Wallis test was performed for anti-CCR4-DT treatment, and a Friedman test was performed for the other treatments. $P < 0.05$ (bold) values were considered significant.

and 20 dpt, statistical significance being only achieved with the high-dose IL-2-DT (P = 0.0029), and trends being seen in the animals receiving the anti-CCR4-DT and low-dose IL-2-DT treatments (Fig. 3F). HLA-DR and CD38 coexpression then rapidly returned to pretreatment levels.

In the LNs, HLA-DR and CD38 coexpression increased on both CD4$^+$ and CD8$^+$ T cells only after the low-dose IL-2-DT administration (Fig. 4C and D), and reached significance only for CD8$^+$ T cells (P = 0.0107) (Fig. 4D). Such increases did not occur after anti-CCR4-DT administration (Fig. 4C and D).

Similarly, in the gut, HLA-DR and CD38 coexpression on T cells increased only minimally after anti-CCR4-DT (Fig. 4G and H) but more dramatically following the low-dose IL-2-DT administration (Fig. 4G and H).

We next assessed the impact of the different Treg depletion strategies on the levels of plasma cytokines, to monitor the levels of systemic inflammation. Inflammatory cytokines IL-15, IL-17, and CXCL-10 (IP-10) increased following every treatment (Fig. 5). Large, but transient, increases of plasma IL-15, peaking at 5 dpt and normalizing by 10 dpt were observed after the administration of high-dose IL-2-DT (Fig. 5A). Conversely, anti-CCR4-DT only induced minimal changes in the plasma levels of IL-15, which may explain why there was only a minimal boost in SIV-specific T cell responses with this treatment (Fig. 5A). IL-17 showed minimal changes with all treatments, with the exception of high-dose IL-2-DT treatment, where IL-17 significantly increased between 3 and 10 dpt (Fig. 5B). A very large increase in IP-10 of up to 600-fold was seen with high-dose IL-2-DT treatment, with only mild increases (up to 10-fold) occurring after the other treatments (Fig. 5C).

Viral reactivation. One hundred per cent of the RMs infected with SIVsab spontaneously control the virus to <1 vRNA copy/ml of plasma (61). Viral reactivation was assessed by measuring SIV plasma VLs by qPCR. Detectable plasma viremia occurred systematically after IL-2-DT administration. In our study design, viral reactivation occurred in the absence of ART in all three animals that received the high-dose IL-2-DT, and one which received the low-dose of IL-2-DT, which enabled additional cycles of viral replication, as documented by the dynamics of the plasma viral loads (pVLs), which peaked at 3 to 4 logs/ml between 10 and 17 dpt (Fig. 6A). Conversely, after administration of the anti-CCR4-DT, no pVLs could be detected (Fig. 6A).

We further assessed the levels of virus reactivation by quantifying the levels of peripheral blood mononuclear cell (PBMC)-associated SIV RNA (CA-vRNA). No significant changes were observed in the CA-vRNA (Fig. 6B), after any of the Treg-depleting treatments, not even in the animals which had plasma viral reactivation. Of note, an increase of about 2-log viral copies/million cells was seen in RM39 following low-dose IL-2-DT, which could indicate a minimal level of cellular reactivation.

Similarly, no significant changes in the levels of the integrated PBMC-associated SIV DNA (CA-DNA) were observed to occur following any treatment (Fig. 6C), further supporting that the levels of virus reactivation after these treatments were relatively low.

Toxicity. The toxicity of the Treg-depleting immunotoxins was assessed after each treatment by measuring serum aspartate transaminase (AST) and serum aminotransaminase (ALT) for liver function, serum urea and serum creatinine for kidney function, and serum albumin to assess for capillary leak syndrome. Minimal level of transient hepatotoxicity was seen with all immunotoxins (Fig. 7A and B). The maximum increase in AST (3.5-fold increase from the baseline) was seen after the administration of the high-dose IL-2-DT. AST increases after the other treatments were <3-fold on average (Fig. 7A). Approximately 4-fold increases in ALT was seen after both IL-2-DT treatments (Fig. 7B). All AST and ALT levels returned to baseline 10 dpt in all treatments (Fig. 7A and B).

Serum urea and creatinine were slightly increased after the administration of the high-dose IL-2-DT and returned to pretreatment levels by 14 dpt (Fig. 7C and D). No
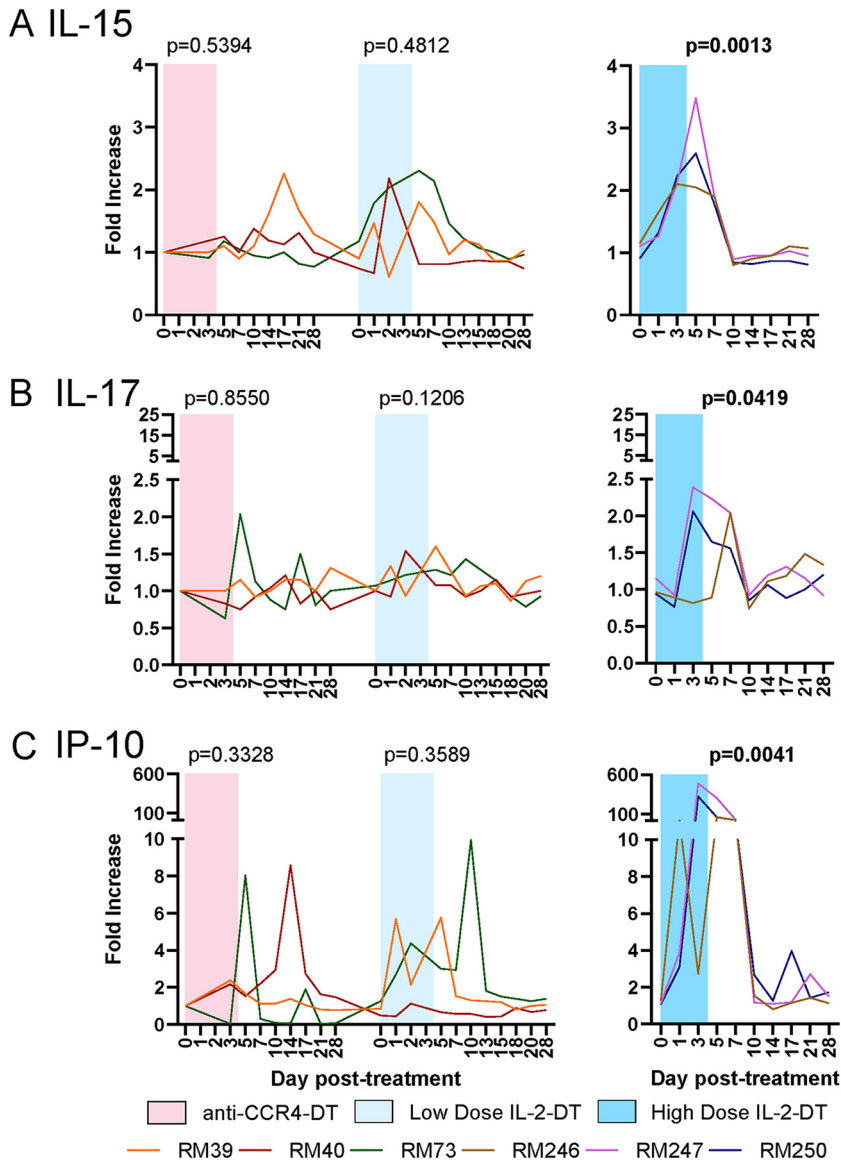
FIG 5 Dynamics of inflammatory cytokines following the administration of the Treg-depleting agents. (A to C) Fold changes in serum IL-15 (A), serum IL-17 (B), and serum IP-10 (C) in treatment with anti-CCR4-DT, low-dose IL-2-DT, and high-dose IL-2-DT. Different treatments are color-coded. The y axes illustrate the fold increase in the levels of cytokines; the x axes illustrate the number of days post-DT administration. A Friedman test was performed individually for each treatment, and $P < 0.05$ (bold) values were considered significant.

discernible elevations occurred with the other treatments (Fig. 7C and D). Minimal alterations in serum albumin were seen with all treatments (Fig. 7E).

SIV-specific T cell responses. One of the premises of our approach was that Treg depletion will boost SIV-specific immune responses and thus the clearance of the reactivated virus. We assessed the changes in SIV-specific T cell responses by stimulating PBMCs isolated at various time points during the follow-up—pretreatment, at treatment completion (4 to 7 dpt), and after immune recovery (28 dpt)—using an SIVsab Gag peptide pool (peptides 69 to 136) and assessing the expression of IL-2, IFN-γ, MIP-1β, TNF-α, and CD107a. While the changes in polyfunctionality were minimal, total cytokine production by CD8+ T cells increased with all treatments, the most profound increase being observed in the group receiving the high-dose IL-2-DT, which was largely due to an increase in CD107a expression (Fig. 8). Following immune
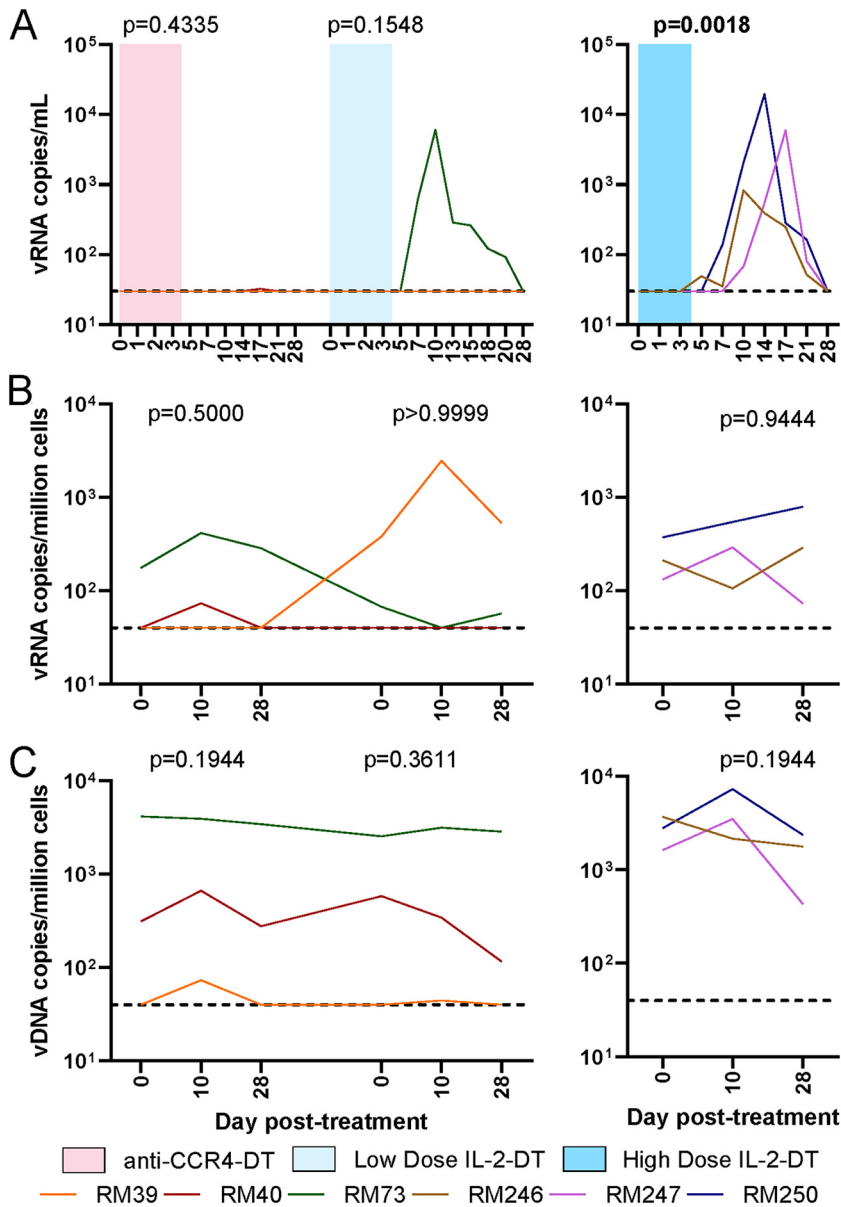
FIG 6 Impact of the different Treg depletion strategies on the virus levels in SIVsab-infected RMs. (A) Plasma viral load (VL) dynamics after administration of anti-CCR4-DT, low-dose IL-2-DT, and high-dose IL-2-DT. (B) PBMC-associated viral RNA (vRNA) copies/million cells after the administration of anti-CCR4-DT, low-dose IL-2-DT, and high-dose IL-2-DT. (C) PBMC-associated vDNA copies/million cells after the administration of anti-CCR4-DT, low-dose IL-2-DT, and high-dose IL-2-DT. Different treatments are color-coded. The y axes illustrate the levels of vRNA or vDNA; the x axes illustrate the number of days post-DT administration. The limit of detection for the plasma VL assay was 30 copies/ml. A Friedman test was performed individually for each treatment, and $P < 0.05$ (bold) values were considered significant.

recovery, the SIV-specific immune responses returned close the pretreatment levels, yet remaining slightly elevated (Fig. 8). Similarly, while upon stimulation with the peptide pool minimal changes in polyfunctionality were observed, the total cytokine production by the CD4$^+$ T cells increase after all treatments, again returning to levels that were slightly higher than the baseline (Fig. 9).

Combination therapy. Since both immunotoxins exerted significant effects on Tregs but only depleted a fraction of this cell subset, we next assessed them in combination to assess whether or not a more prominent depletion would improved the observed effects on the virus reactivation and boosting of the cellular immune responses. We first used a combination of anti-CCR4-DT and IL-2-DT, in a ratio of 1.62:1
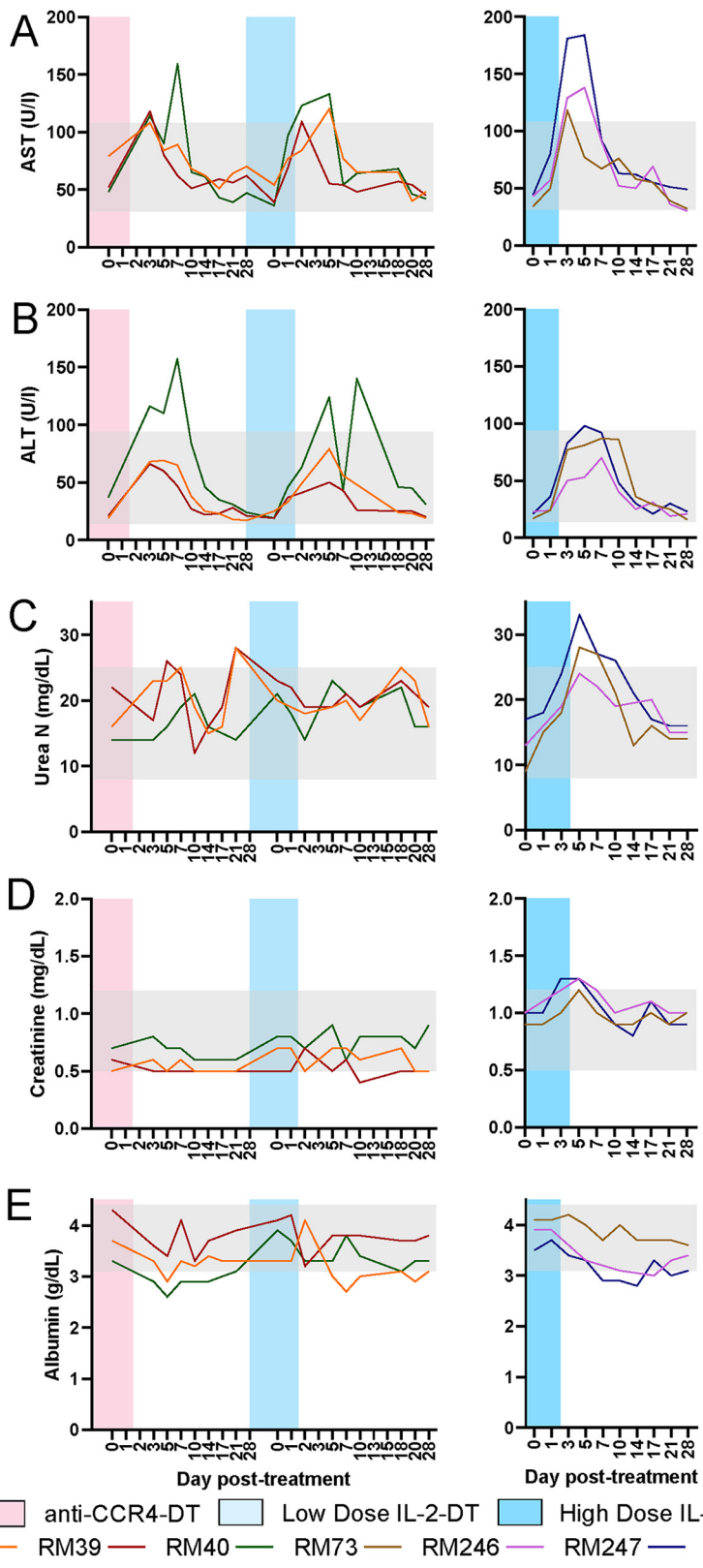
FIG 7 Assessment of drug toxicities after administration of various Treg-depleting immunotoxins. (A to E) Serum levels of AST (A), ALT (B), urea (C), creatinine (D), and albumin (E) after the administration of anti-CCR4-DT and low-dose IL-2-DT and high-dose IL-2-DT. The y axes illustrate the levels of the tested biomarker; the x axes illustrate the number of days post-DT administration. Gray areas illustrate the normal values.
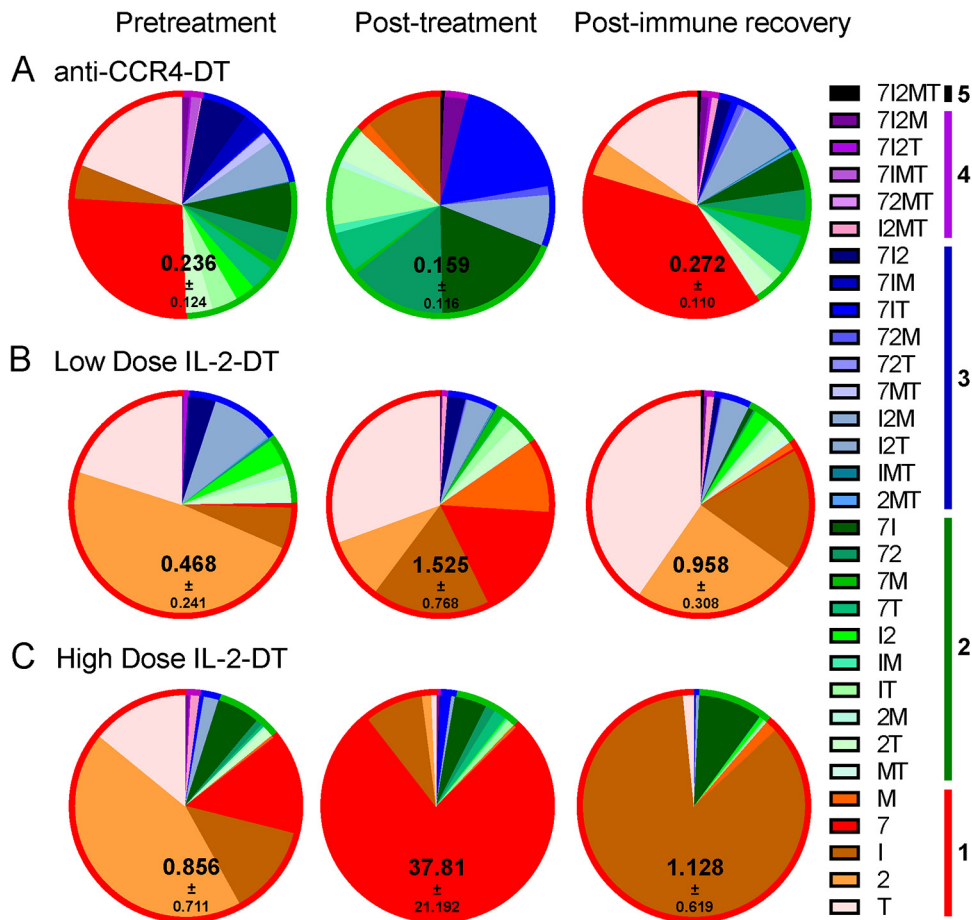
FIG 8 (A to C) Changes in the frequency of the SIV-specific CD8$^+$ T cells after the administration of the anti-CCR4-DT (A), low-dose IL-2-DT (B), and high-dose IL-2-DT (C). SIV-specific CD8$^+$ T cells were assessed based on the expression of IFN-γ, IL-2, MIP-1β, TNF-α, and CD107a. Both the individual expression of the specificities and their combinations were assessed, as illustrated in the legend. Polyspecificities are illustrated as circles around the SIV-specific responses. The mean of the sum of total expression with the standard error of the mean (SEM) is presented within each pie.

by weight (Combo-DT1), and administered as a total of 25 μg/kg, i.v., BID for 5 days, and a reversed ratio of the anti-CCR4-DT and IL-2-DT drug combination to 1:1.62 (Combo-DT2), and tried a different dosing regimen of 50 μg/kg, i.v., BID on the first day, and 25 μg/kg, i.v., BID for 6 days.

Significant Treg depletion was observed to occur after the administration of the Combo-DT1, which did not occur after the administration of the Combo-DT2 (Fig. 10A). In the superficial LNs, similar to the previous treatments, more than 32 to 52% of Tregs were depleted after the administration of the combination treatments (Fig. 10B), yet not reaching statistical significance. In the gut, surprisingly, the administration of Combo-DT1 resulted in an increase of the mucosal Tregs, while the administration of Combo-DT2 induced only minimal alterations of the Treg population (Fig. 10C). As with the other treatments, total CD4$^+$ T cell counts were moderately reduced after the administration of the combination treatments, followed by a rapid rebound by 10 to 14 dpt and stabilization to pretreatment levels by 21 to 28 dpt (Fig. 10D). However, these changes were not statistically significant with Combo-DT2. Both of the combination treatments impacted the CD8$^+$ T cell counts, with significance being reached after the administration of the Combo-DT1 (Fig. 10E).

Similar to the other treatments, there was a dramatic increase in the circulating T cell fraction expressing K_i-67 after the administration of combination treatments, which peaked between 10 and 14 dpt, reaching levels representing up to 30 to 80% of
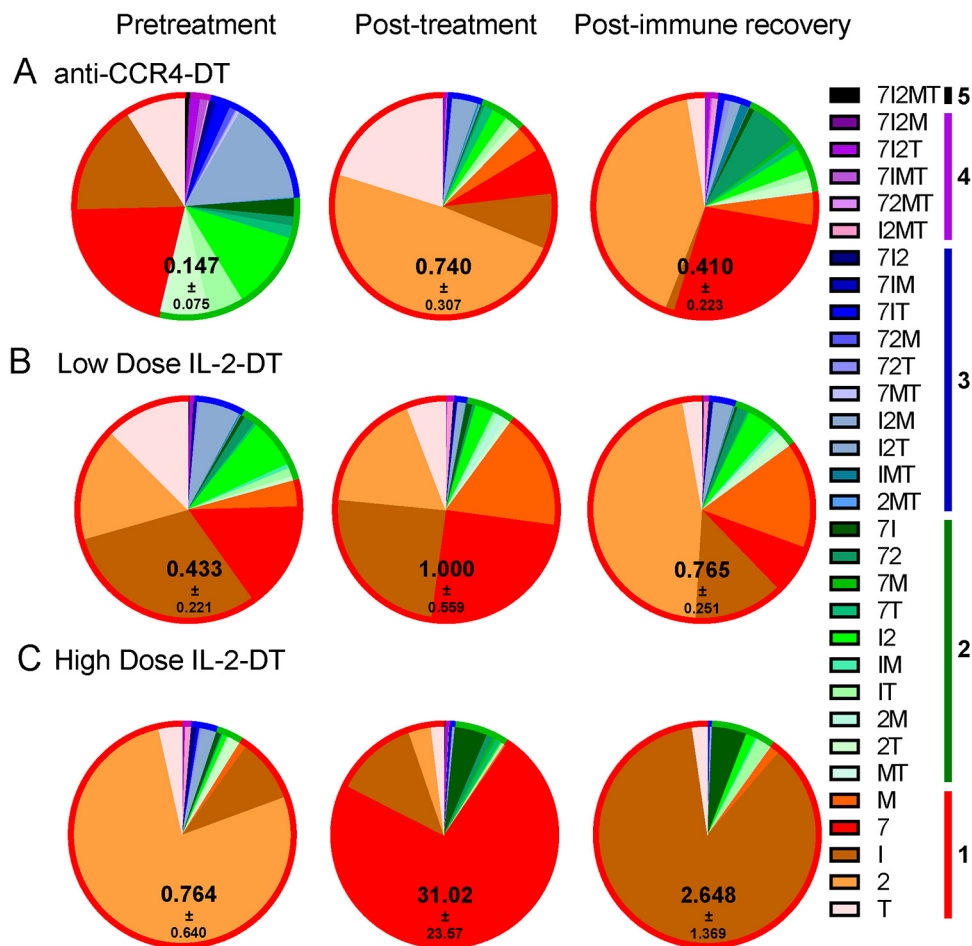
FIG 9 (A to C) Changes in the frequency of the SIV-specific CD4$^+$ T cells after the administration of the anti-CCR4-DT (A), low-dose IL-2-DT (B), and high-dose IL-2-DT (C). SIV-specific CD4$^+$ T cells were assessed based on the expression of IFN-γ, IL-2, MIP-1β, TNF-α, and CD107a. Both the individual expression of the specificities and their combinations were assessed, as illustrated in the legend. Polyspecificities are illustrated as circles around the SIV-specific responses. The mean of the sum of total expression with the SEM is presented within each pie.

circulating CD4$^+$ T cells (Fig. 10F) and 60 to 80% of circulating CD8$^+$ T cells (Fig. 10G), with only the changes with Combo-DT1 reaching statistical significance. Plasma levels of inflammatory cytokines IL-15, IL-17, and CXCL-10 (IP-10) occurred following the administration of the combination treatments (Fig. 10H to J). Large, but transient, increases of plasma IL-15, peaking 5 dpt and normalizing by 10 dpt were observed after the administration Combo-DT1 (Fig. 10H). Conversely, Combo-DT2 only induced minimal changes in the plasma levels of IL-15 (Fig. 10H). IL-17 showed minimal changes with both treatments (Fig. 10I). A mild increase in IP-10 (up to 10-fold) occurred after both treatments (Fig. 10J).

A minimal level of transient hepatotoxicity occurred after the administration of the combo therapies (Fig. 11A and B). Thus, AST levels increases up to 3-fold the average levels (Fig. 11A). Meanwhile, ALT levels increased ~4-fold after the administration of the Combo-DT1 treatment (Fig. 11B). In both cases, AST and ALT levels returned to baseline 10 dpt (Fig. 11A and B). No discernible elevations occurred in serum urea and creatinine with the combination treatments (Fig. 11C and D).

One of the RMs was sacrificed 28 dpt after the Combo-DT1 treatment due to clinical deterioration. This RM presented with low levels of serum albumin, which reached 2.3 g/dl at sacrifice (Fig. 11E), indicating a rare fatal adverse reaction, called capillary leak syndrome, which was previously reported to occur as a result of IL-2-DT administration (67, 68). Serum albumin levels were stable in all other RMs throughout different treatments and follow-up (Fig. 7E and 11E).
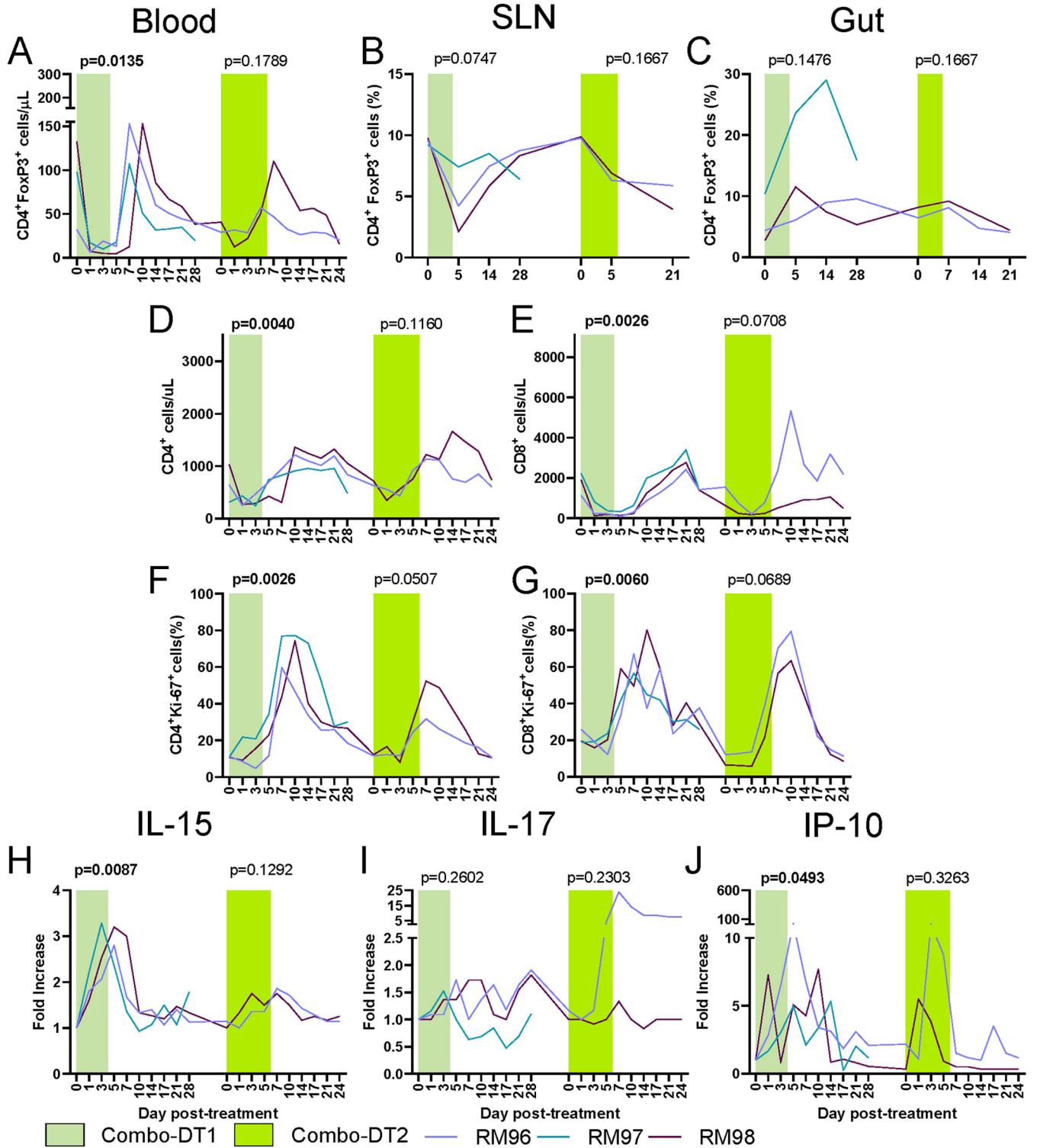
FIG 10 (A to C) Treg (FoxP3^{high} CD4^{+} T cells) dynamics in circulation (A), superficial lymph nodes (B), and intestine (C) on treatment with a combination of anti-CCR4-DT and IL-2-DT, in a ratio of 1.62:1 by weight (Combo-DT1), and in a ratio of 1:1.62 (Combo-DT2). (D and E) Dynamics of CD4^{+} T cells (D) and CD8^{+} T cells (E) after administration of the Combo-DT1 and Combo-DT2 treatments. (F and G) Dynamics of T cell immune activation, as assessed by the changes in the frequency of K_i-67 expression by the circulating CD4^{+} (F) and CD8^{+} (G) T cells. (H to J) Fold changes in serum IL-15 (H), serum IL-17 (I), and serum IP-10 (J) after administration of the Combo-DT1 and Combo-DT2 treatments. A Friedman test was performed, and $P < 0.05$ (boldface) values were considered significant.
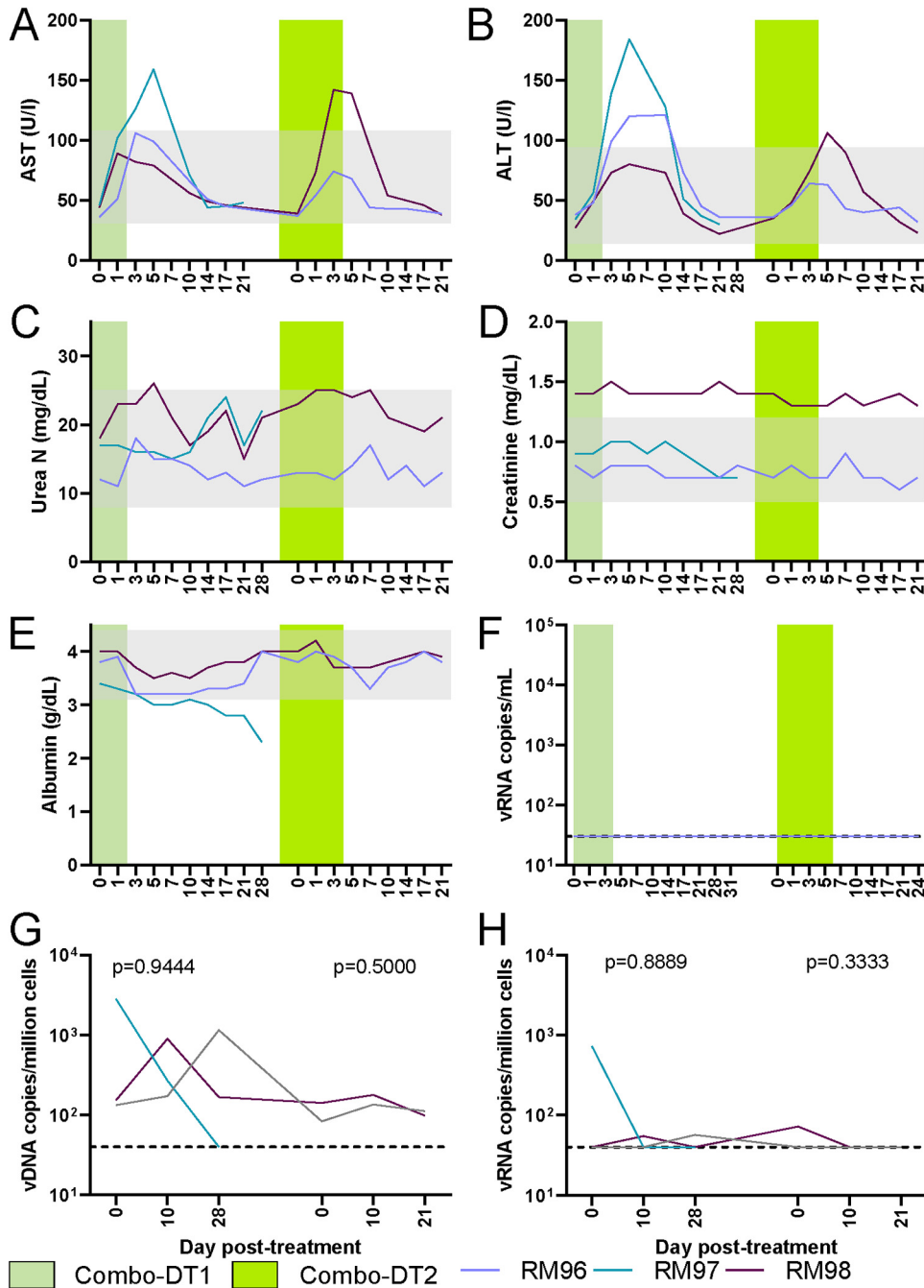
FIG 11 (A to F) Assessment of drug toxicity after the administration of a combination of anti-CCR4-DT and IL-2-DT, in a ratio of 1.62:1 by weight (Combo-DT1), and in a ratio of 1:1.62 (Combo-DT2), through the dynamics of serum AST (A), ALT (B), urea (C), creatinine (D), and albumin (E). (F) Dynamics of virus reactivation in plasma (vRNA copies/ml of plasma) (F), PBMC-associated viral DNA (vDNA) copies/million cells (G), and PBMC-associated vRNA copies/million cells (H). Gray regions are normal values for chemistry parameters. The limit of detection for the plasma VL assay is 30 copies/ml.

After administration of the combo therapies, no pVLs could be detected (Fig. 11F). Furthermore, no significant changes were observed in the CA-vRNA or CA-DNA with the combo therapies (Fig. 11G and H).

Upon stimulation with the peptide pool, the total cytokine production by CD8^{+} T cells increased with Combo-DT1 treatment only, although the changes in polyfunctionality were minimal. Similar to the previous treatments, following immune recovery, the SIV-specific immune responses returned close to the pretreatment levels, yet
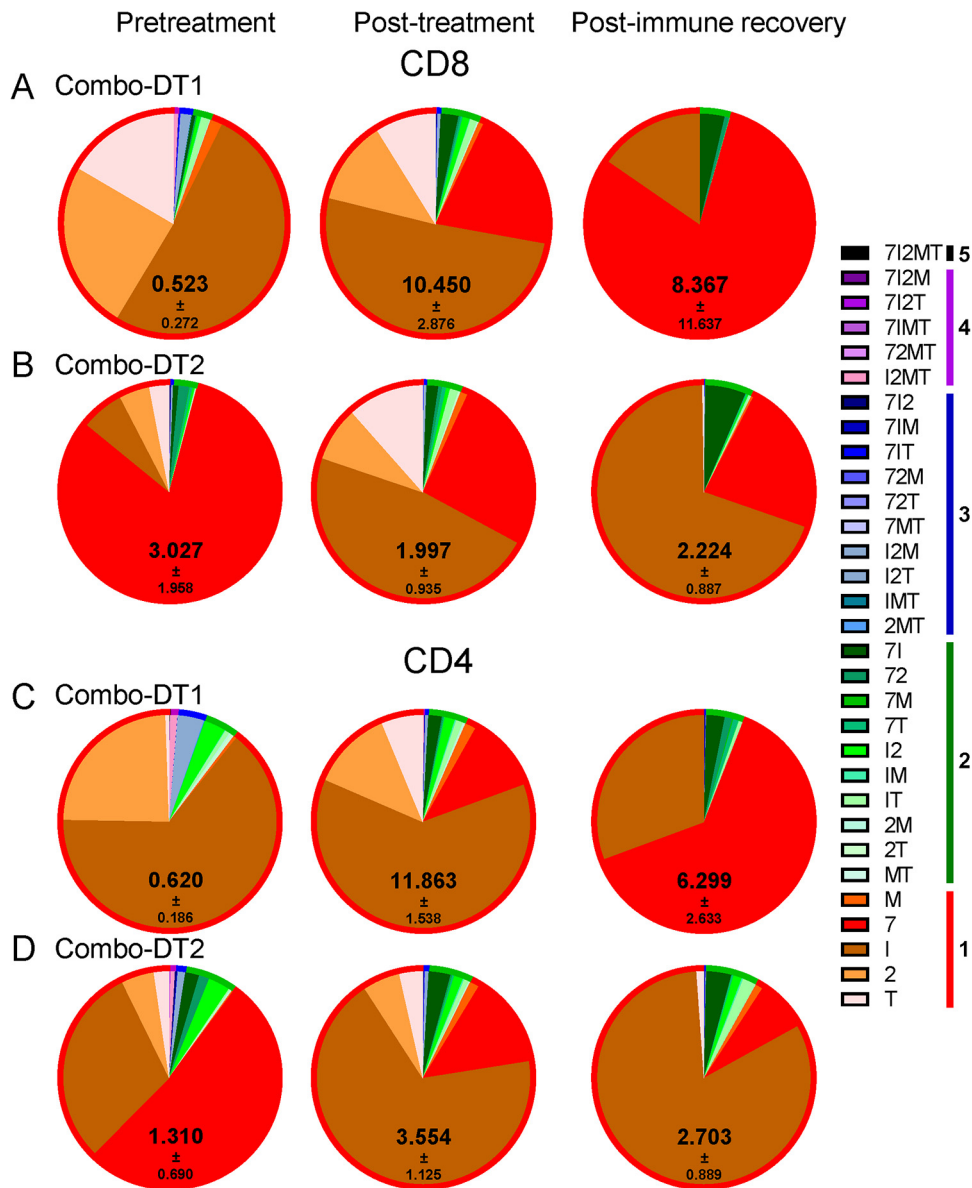
FIG 12 (A to D) Changes in the frequency of the SIV-specific CD8^{+} and CD4^{+} T cells after the administration of a combination of anti-CCR4-DT and IL-2-DT, in a ratio of 1.62:1 by weight (Combo-DT1) (A and C), and in a ratio of 1:1.62 (Combo-DT2) (B and D). SIV-specific T cells were assessed based on the expression of IFN-γ, IL-2, MIP-1β, TNF-α, and CD107a. Both the individual expression of the specificities and their combinations were assessed, as illustrated in the legend. Polyspecificities are illustrated as circles around the SIV-specific responses. The mean of the sum of total expression with the SEM is presented within each pie.

remaining slightly elevated (Fig. 12A and B). Similarly, upon stimulation with the peptide pool, minimal changes in the CD4^{+} T cell polyfunctionality were seen; however, total cytokine production by the CD4^{+} T cells increased after both combo treatments, again returning to levels that were slightly higher than the baseline (Fig. 12C and D).

IL-2-DT with ART. Since our best results were obtained with the IL-2-DT administration, we next assessed the efficacy of this Treg depletion strategy in an environment which is relevant for people living with HIV, i.e., in chronically SIV-infected RMs on ART. We proceeded to use low-dose IL-2-DT (25 μg/kg, i.v., BID) as a precaution for drug interactions with ART. Five RMs were infected with SIVsab and allowed to spontaneously control the virus. After maintenance of the complete viral suppression for more than 1 year, ART was initiated in all the RMs with the TDF+FTC+DTG coformulation (64)
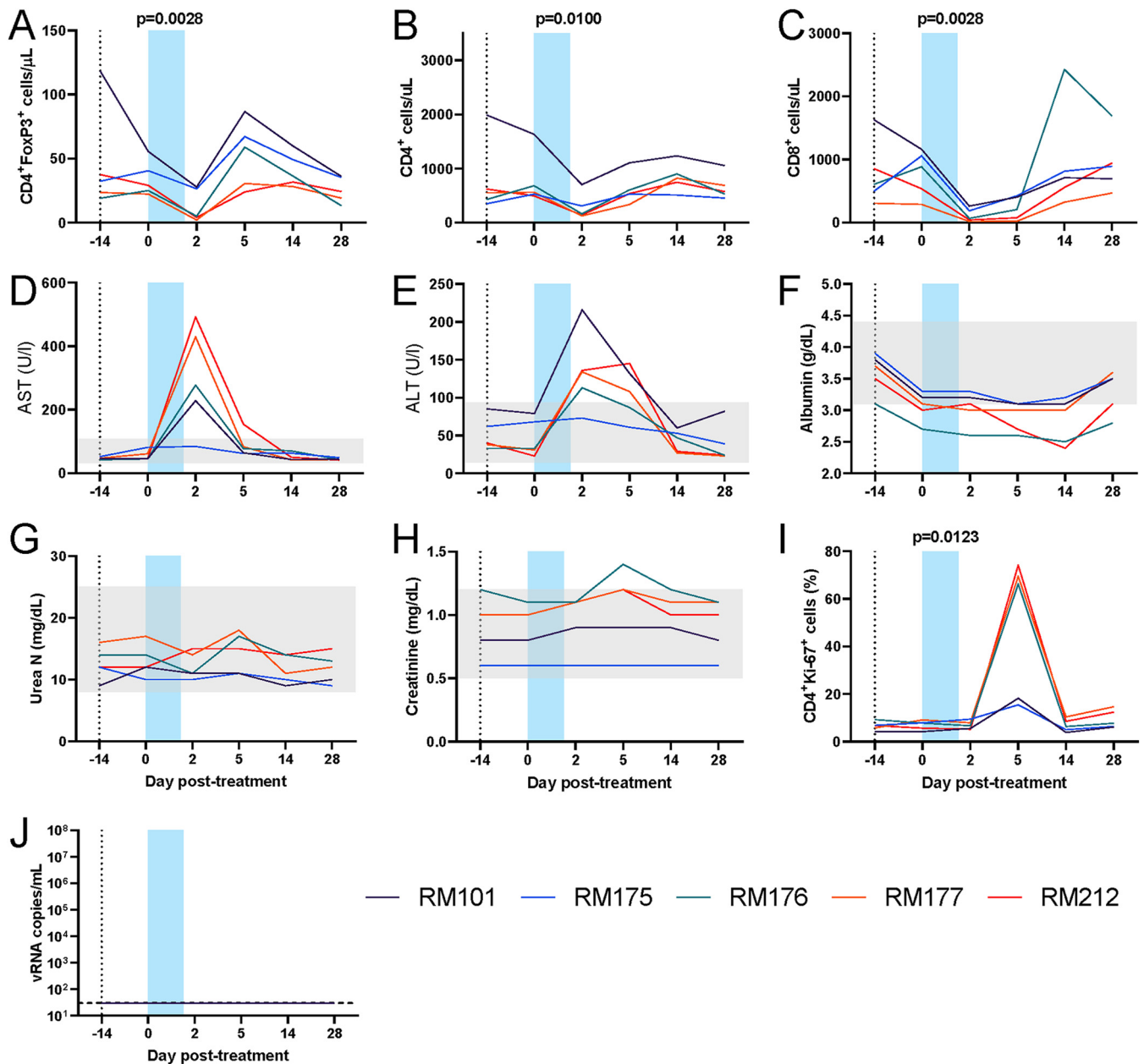
FIG 13 Treg depletion with a low-dose IL-2-DT in SIV-infected rhesus macaques on ART. (A to C) Dynamics of the circulating Tregs (FoxP3^{high} CD4$^+$ T cells) (A), CD4$^+$ T cells (B), and CD8$^+$ T cells (C). (D to H) Assessment of drug toxicity through the dynamics of serum AST (D), ALT (E), albumin (F), urea (G), and creatinine (H). (I) Dynamics of T cell immune activation, as assessed by the changes in the frequency of K_i-67 expression by the circulating CD4$^+$ T cells. (J) Dynamics of virus reactivation in plasma (vRNA copies/ml of plasma). Gray regions are normal values for chemistry parameters. The limit of detection for the plasma VL assay is 30 copies/ml. A Friedman test was performed, and $P < 0.05$ (boldface) values were considered significant.

for 14 days, followed by low-dose IL-2-DT administration (25 μg/kg, i.v., BID). Unfortunately, after the third IL-2-DT administration, this treatment had to be suspended because four of the five RMs had severe clinical signs of discomfort (decreased appetite, bruising on the legs, not alert and responsive, sitting or lying down in the cage).

Analyses of the data collected prior to treatment interruption showed that four of five RMs depleted a large fraction of Tregs (Fig. 13A). However, this depletion occurred in the context of dramatic decreases of both CD4$^+$ and CD8$^+$ T cells that resulted in severe lymphopenia (Fig. 13B and C). Toxicity studies found an average 6-fold elevation of AST (highest, 10.9-fold) in four of five animals (Fig. 13D) and an average 3.6-fold elevation of ALT (highest, 5.9-fold) (Fig. 13E), which occurred at 2 dpt. However,

although their serum albumin levels decreased, they did not dip below 2 g/dl and recovered rapidly, suggesting that the adverse clinical signs were not due to capillary leak syndrome (Fig. 13F). Serum urea and creatinine levels were not altered upon IL-2-DT and ART administration (Fig. 13G and H). Three of five animals showed large increases in T cell activation (i.e., 74% of the CD4$^+$ T cells expressed K_i-67) at 5 dpt (Fig. 13I). No detectable levels of plasma virus were observed in any of the animals in spite of these high levels of T cell immune activation (Fig. 13I).

DISCUSSION

In this study, we tested multiple therapeutic approaches to deplete Tregs as a new cure strategy aimed at reactivating SIV from latency and improving the clearance of SIV-infected cells upon reactivation. Development of such an improved strategy is justified by the limitations of currently available LRAs, which have shown poor efficacy in reversing latency and reactivating the reservoir (13, 14). This is further compounded by the daunting observation that, even if such an effective LRA would exist, the exhausted cellular immune effectors are largely inefficient in effectively clearing the infected cells (10).

Therefore, we postulated that Treg depletion in SIV-infected RMs on ART may represent a sound new strategy toward an HIV cure because, through a single intervention, we can achieve virus reactivation, a boost of SIV-specific responses, and a direct reduction of the reservoir size (27). To this goal, we tested multiple Treg depletion strategies. The need for these multiple approaches is justified by the lack of specificity of the surface markers for Treg identification. The current standard Treg marker (FoxP3) is intracellular and therefore cannot be targeted *in vivo*.

We thus focused on two surrogate markers: CD25, which is the IL-2 receptor which present on a majority of Tregs, and CCR4, which is a receptor of CCL17/CCL22 and is present on effector Tregs. We reasoned that the fact that either IL-2-DT or anti-CCR4-DT induce only an incomplete Treg depletion is not necessarily a pitfall of our approach, since even a partial depletion would curb the reservoir and impair Treg functions, as suggested by our previous studies (27). In fact, we reasoned that an incomplete Treg depletion is desirable because a complete Treg depletion may induce autoimmunity, as suggested by the very severe autoimmune and inflammatory disorders in human newborns without functional Tregs (53, 54). Nevertheless, to expand our ability to deplete Tregs, we also used combinations of IL-2-DT and anti-CCR4-DT in two different ratios.

All the therapeutic regimens used in our study depleted between 85% (high-dose IL-2-DT and Combo-DT1 treatment) and 30% (Combo-DT2 treatment) of circulating Tregs. In none of the approaches was Treg depletion either complete or long term. In fact, soon after the transient depletion of Tregs, a rapid rebound was observed, which was probably due to generalized activation of the T cells causing both proliferation of the residual Tregs and conversion of the CD4$^+$ T cells to a Treg phenotype. While Tregs were most effectively depleted from circulation, a certain depletion also occurred in the LNs and the gut as well. Interestingly, the most prominent mucosal Treg depletion occurred after the IL-2-DT treatment, which was also the treatment that resulted in the most prominent plasma VL rebound and increase in SIV-specific cellular response. This may indicate that the observed viral reactivation occurred in the infected cells in the gut. Of note, an unexpected Treg increase was observed in the gut after the Combo-DT1 treatment, which could be due to an earlier rebound of Tregs compared to the other treatments, or to a less effective Treg depletion.

Meanwhile, all of the therapeutic attempts to deplete Tregs resulted in a nonnegligible depletion of the overall CD4$^+$ and CD8$^+$ T cell populations. They were both transient and, as expected, were followed by significant increases in the CD4$^+$ and CD8$^+$ T cell counts.

Unfortunately, the first premise of our hypothesis, i.e., that Treg depletion will curb the SIV reservoir, was not achieved by any of the proposed treatments. Indeed, monitoring the CA-vDNA did not show any significant change throughout the treat-

ment, with any of the treatments administered. While a reduction in both Treg and total CD4$^+$ T cell populations was observed, it was not of the magnitude expected to exert a significant impact on the reservoir, particularly due to the fact that depletion mainly involved circulating Tregs and less so the LN or mucosal Tregs.

The second premise, i.e., that the therapeutic agents used for Treg depletion reactivate viral reservoir and that they are more effective than the currently available LRAs, proved only partially correct. The immunotoxins based on the use of IL-2 were indeed relatively successful in inducing viral reactivation through a massive increase in CD4$^+$ and CD8$^+$ T cell activation, which were associated with massive increases in proinflammatory cytokines and chemokines, such as IL-15, IL-17, and IP-10. IL-15 promotes survival, proliferation, and effector function of cytotoxic T lymphocytes in the presence of Tregs (69). The plasma IL-15 increases were also associated with the largest boosts in SIV-specific T cell responses. Similarly, since Tregs reduce IP-10 production (70), the observed IP-10 increase could have been triggered by the Treg depletion. In agreement with the massive increases in immune activation observed after IL-2-DT administration, viral reactivation occurred only after the IL-2-DT administration, being likely secondary to the massive T cell activation induced by IL-2. This interpretation is supported by the observation that in the combination treatments, in which we observed similar levels of T cell activation to those observed with the IL-2-DT treatment, the virus rebound was either minimal or lacking, probably due to an insufficient amount of IL-2-DT in the combination.

The observation that the levels of PBMC CA-vRNA remained relatively unchanged, even in the RMs which showed plasma reactivation is not surprising, since only a small fraction of PBMCs would need to reactivate for such levels of plasma viremia to occur. Considering a blood volume of 69 ml/kg (71), a 5-kg monkey with a hematocrit of 45% has an overall plasma volume of 217 ml. A pVL of 10^4 viral copies/ml would thus correspond to a total number of 2.2×10^6 viral copies in plasma. With approximately 1,500 virions produced in viral burst from an activated cell (72), a total of 1,467 CD4$^+$ T cells would need to be activated to produce virus. With estimates that circulating lymphocytes represent only 0.3 to 0.5% of the total body lymphocytes (73), this would imply that 4 to 7 circulating reactivated cells contribute to the observed a 4-log pVL. Note that this calculation does not factor in a dynamic viral production that would generate the observed amounts of virus progressively. As such, the minimal changes in the PBMC levels of CA-vRNA and CA-vDNA are expected, and thus, the second premise of our study was only partial achieved through Treg depletion.

Interestingly, IL-2-DT induced a significant increase of Treg activation, in addition to other T cell subsets, as illustrated by the increases in CD39 and CD73, two ectonucleases which hydrolyze ATP to AMP and contribute to the immunosuppressive function of Tregs (66, 74–76). Yet, despite an increase of the Treg suppressive function, IL-2-DT was also associated an increase in SIV-specific immune response, probably resulting from the decrease in the overall Treg counts. The boost of the SIV-specific responses was relatively short-lived, mirroring the relative rapid restoration of Tregs and their suppressive function.

As such, our results suggest that we accomplished our third goal, i.e., boosting the T cell immune responses to clear the infected cells. Interestingly, SIV-specific T cell responses were boosted even by those treatments where no plasma viral reactivation was observed. Also, in the treatments that induced viral reactivation, the SIV-specific response increased prior to virus becoming detectable in plasma, and thus we concluded that they are a direct result of Treg depletion and not of exposure to the viral particles. This suggested that even if a potent viral reactivation could not be achieved in every instance of Treg depletion, the use of Treg-depleting agents could have potential for cure prospects when combined with other potent LRAs.

This prompted us to test our strategy in a model of chronic HIV infection, SIV-infected RMs on ART. RM controllers were placed on ART for 14 days prior to treatment and then IL-2-DT therapy was initiated. Our choice was justified by our results in the naive controllers showing that this approach accomplishes most of our goals (i.e., the

maximal Treg depletion, virus reactivation, and a significant boost of the SIV-specific T cells). Yet, in this setting, IL-2-DT administration had to be discontinued after only three doses, due to severe hepatotoxicity in 4/5 treated animals. Since we did not observe such toxicity when administering IL-2-DT to SIV-infected naive RMs, we concluded that the association between ART and IL-2-DT is the reason for this massive toxicity, and we discontinued the treatments. Even more daunting, in RMs on ART that received IL-2-DT, we observed a significant lymphopenia, which involved all the T lymphocyte subsets, including the SIV-specific T cells. Such a massive impact on the SIV-specific immune responses countered the boost observed in naive animals, thus offsetting one of the main premises of our approach.

Therefore, our overall conclusion is that the proposed strategy of Treg depletion with IL-2-DT is not feasible in individuals on ART, which calls for different approaches. Several alternative treatments depleting Tregs are available, including low-dose cyclophosphamide, daclizumab, zoledronic acid (45, 77), and treatments to modify Treg function through CTLA4 blockade (78, 79). These agents will need to first be assessed for drug interactions with ART and then tried in the setting of SIV/HIV infection on ART to assess whether Treg depletion can increase virus specific cellular responses and virus reactivation. Should such an effect be observed, combinations with potent LRAs may improve the current strategies. Based on the current data, Treg targeting as a strategy for HIV cure cannot be discarded.

MATERIALS AND METHODS

Animals, infection, and treatments. Fourteen RMs of Indian origin (*Macaca mulatta*) were i.v. infected with 300 50% tissue culture infectious doses ($TCID_{50}$) of SIVsab92018 (80, 81) and allowed to naturally control infection. In this model, complete immunological and viral suppression occurs in 100% of animals, which maintain persistent reservoirs with replication competent virus (61, 82); this permits screening of reservoir reactivation strategies without the multidrug ART confounding factor.

All animals were housed and maintained at the Plum Borough Research animal facility of the University of Pittsburgh according to the standards of the Association for Assessment and Accreditation of Laboratory Animal Care (AAALAC), and experiments were approved by the University of Pittsburgh Institutional Animal Care and Use Committee (IACUC; protocols 16027641 and 19014354). The animals were fed and housed according to regulations set forth by the *Guide for the Care and Use of Laboratory Animals* and the Animal Welfare Act (83). All RMs included in this study were socially housed (paired) indoors in stainless steel cages, had a 12/12 light cycle, and were fed twice daily; water was provided *ad libitum*. A variety of environmental enrichment strategies were employed, including housing of animals in pairs, providing toys to manipulate and playing entertainment videos in the animal rooms. In addition, the animals were observed twice daily, and any signs of disease or discomfort were reported to the veterinary staff for evaluation. For sample collection, animals were anesthetized with 10 mg/kg ketamine HCl (Park-Davis, Morris Plains, NJ) or 0.7 mg/kg tiletamine HCl and zolazepan (Telazol; Fort Dodge Animal Health, Fort Dodge, IA) injected intramuscularly. At the study completion, the animals were sacrificed by i.v. administration of barbiturates. Five RMs received coformulated ART (64) initiated 14 days prior to immunotoxin administration.

Treg depletion. Was performed with anti-CCR4-DT and IL-2-DT, or their combinations, as detailed below. Immunotoxins were prepared as described previously (84).

CCR4 is a surface marker found on effector Tregs (85). The anti-human CCR4-DT has been effectively used to deplete Tregs in pigs (86), NHPs (63, 87), and in human CCR4$^+$ tumor-bearing mouse models (88).

IL-2-DT was previously commercially produced as Ontak, a U.S. Food and Drug Administration-approved chemotherapeutic drug used for CD25$^+$ cutaneous T cell lymphoma (89) and found to be relatively effective in treating peripheral T cell lymphoma, metastatic renal cell carcinoma, and unresectable stage IV melanoma (90–92). However, Ontak was discontinued due to difficulty with purification in the *Escherichia coli* expression system. A new antihuman IL-2-DT, with a yeast expression system, has been synthesized and shown to work both *in vitro* and in a human CD25$^+$ tumor bearing mouse model (59, 84).

Five treatment conditions were tested to deplete Tregs, including different doses and/or combinations of IL-2-DT, anti-CCR4-DT, and the combination of these, as follows: (i) anti-CCR4-DT, which was administered i.v., at a dose of 25 μg/kg, BID for 5 days to three SIVsab-infected RMs; (ii) these RMs also received a low i.v. dose of 25 μg/kg of IL-2-DT, BID for 5 days; (iii) a high i.v. dose of 35 μg/kg of IL-2-DT was administered BID for 5 days to three SIVsab-infected RMs; (iv) a combination of anti-CCR4-DT and IL-2-DT in a ratio of 1.62:1 by weight was administered as a total of 25 μg/kg, i.v., BID for 5 days to three SIVsab-infected RMs; and (v) two animals received a reversed ratio of the drug combination to anti-CCR4-DT and IL-2-DT at 1:1.62, with a dosing regimen of 50 μg/kg, i.v., BID on the first day and 25 μg/kg i.v., BID for 6 days (63). Blood, superficial LN biopsy specimens, and intestinal biopsy specimens were collected for both treatments.

Treg depletion in the setting of ART was tested in 5 SIVsab-infected RMs. After 14 days of subcutaneous administration of TDF+FTC+DTG coformulated ART (64), IL-2-DT was administered at a dose of

25 μg/kg, i.v., BID. After three doses, treatment was discontinued in four of the five RMs due to clinical signs of discomfort. In the fifth RM (RM101), which was clinically healthy, a fourth dose was administered, but then the treatment was discontinued in this RM as well.

Sample collection and processing. Blood was collected in EDTA anticoagulant collection tubes pretreatment and 1, 3, 5, 7, 10, 14, 17, 21, and 28 dpt. Plasma was separated using centrifugation, and PBMCs were isolated by density gradient separation using lymphocyte separation medium (Lonza, Switzerland). For anti-CCR4-DT treatment, LN biopsy specimens were performed pretreatment (all) and 4 (RM39 and RM73), 7 (RM39 and RM40), 14 (RM40 and RM73), and 21 (all) dpt, and intestinal resections were performed at pretreatment (all) and at 4 (RM40), 7 (RM73), and 14 (RM39) dpt. For the low-dose IL-2DT treatment, LN and intestinal biopsies were performed pretreatment and 5 and 28 dpt. For the Combo-DT1, LN and intestinal biopsy specimens were collected pretreatment and 5, 14, and 28 dpt. For the Combo-DT2, LNs were collected pretreatment and 5 and 21 dpt, and intestinal biopsy specimens were collected pretreatment and 7, 14, and 21 dpt. Cells were isolated from tissues as previously described (49, 81, 82, 93).

Flow cytometry. Whole blood and mononuclear cells isolated from the LNs or intestine were stained for flow cytometry, as described previously (80). Staining for FoxP3 was performed using a FoxP3 Fix/Perm buffer set (BioLegend, CA) according to the manufacturer's protocol. Intracellular staining for K_i-67 was performed as previously described (94). Stained cells were acquired on an LSR-II flow cytometer (Becton Dickinson [BD], NJ) and analyzed with FlowJo version 10 (TreeStar, OR). Antibodies used were as follows (clones are indicated in parentheses). All antibodies were from BD unless otherwise noted: FoxP3-AF488 (259D; BioLegend, CA), CD25-PE (2A3), CD8-PE-CF594 (RPA-T8), CD95-PE-Cy5 (DX2), CD28 PE-Cy7 (CD28.2), CD4 APC (L200), CD3 V450 (SP34-2), CD39 PE (eBioA1; Invitrogen, CA), CD194 PECy7 (1G1), CD73 PerCP-Cy5.5 (AD2), CD38 FITC (AT-1; Stemcell, Canada), CD69 APC-Cy7 (FN50), K_i-67 PE (B56), HLA-DR PE-Cy7 (L243), and CD45 PerCP (D058-1283).

Trucount (BD) was used to quantify the absolute CD3$^+$ cell counts according to the manufacturer's protocols. Other cell counts were calculated using percentages obtained from other panels on the CD3$^+$ cell count.

Viral quantification. SIV pVLs were measured using quantitative real-time PCR as previously described (80, 95). Cell-associated vRNA and vDNA quantifications were performed by using quantitative PCR (qPCR) on TRIzol-based extractions, as previously described (96). Briefly, the DNA phase was extracted by adding 500 μl of DNA extraction solution (4 M guanidine thiocyanate, 50 mM sodium citrate, 1 M Tris) (97). Extracted plasma RNA samples were reverse-transcribed, and cDNAs and vDNAs were quantified by qPCR using long terminal repeat-specific primers and a labeled probe (80). Viral RNA and DNA copies was divided by the number of cells, as assessed by CCR5-specific primers.

Chemistries. Were tested on serum samples by the Marshfield Laboratories. Normal ranges were determined using a set of 21 uninfected RMs from our colony housed at the same site, since normal ranges of chemistry parameters can vary by colony.

Cytokine testing. Was done on frozen plasma using a 29-plex Luminex (Thermo Fisher, MA) according to the manufacturer's protocol and as previously described (98–100); results were read on a Bio-Plex reader (Bio-Rad Laboratories, CA).

SIV-specific T cell responses. SIV-specific T cell responses were assessed using frozen PBMCs from each treatment. Intracellular staining and flow cytometry analyses were performed as described previously (16, 27), using SIVsab Gag (69 to 136 peptides) peptide pool, on an LSR-II flow cytometer (BD), and analyzed with FlowJo version 10 (TreeStar).

Statistical analysis. A Kruskal-Wallis test was performed for each parameter from intestinal resections and superficial lymph nodes in anti-CCR4-DT treatment. For all others, the Friedman test was used for each parameter for each treatment group to assess whether there was statistical variation in the parameter throughout treatment and follow-up due to the treatment. A P value of <0.05 was considered statistically significant. All statistical testing and graphing were done using Prism 8 (GraphPad, CA).

REFERENCES

1. Chun TW, Fauci AS. 1999. Latent reservoirs of HIV: obstacles to the eradication of virus. Proc Natl Acad Sci U S A 96:10958–10961. https://doi.org/10.1073/pnas.96.20.10958.

2. Siliciano JD, Siliciano RF. 2016. Recent developments in the effort to cure HIV infection: going beyond $N = 1$. J Clin Invest 126:409–414. https://doi.org/10.1172/JCI86047.

3. Finzi D, Blankson J, Siliciano JD, Margolick JB, Chadwick K, Pierson T, Smith K, Lisziewicz J, Lori F, Flexner C, Quinn TC, Chaisson RE, Rosenberg E, Walker B, Gange S, Gallant J, Siliciano RF. 1999. Latent infection of CD4$^+$ T cells provides a mechanism for lifelong persistence of HIV-1, even in patients on effective combination therapy. Nat Med 5:512–517. https://doi.org/10.1038/8394.

4. Siliciano JD, Kajdas J, Finzi D, Quinn TC, Chadwick K, Margolick JB, Kovacs C, Gange SJ, Siliciano RF. 2003. Long-term follow-up studies confirm the stability of the latent reservoir for HIV-1 in resting CD4$^+$ T cells. Nat Med 9:727–728. https://doi.org/10.1038/nm880.

5. Strain MC, Gunthard HF, Havlir DV, Ignacio CC, Smith DM, Leigh-Brown AJ, Macaranas TR, Lam RY, Daly OA, Fischer M, Opravil M, Levine H, Bacheler L, Spina CA, Richman DD, Wong JK. 2003. Heterogeneous clearance rates of long-lived lymphocytes infected with HIV: intrinsic stability predicts lifelong persistence. Proc Natl Acad Sci U S A 100:4819–4824. https://doi.org/10.1073/pnas.0736332100.

6. Wong JK, Hezareh M, Gunthard HF, Havlir DV, Ignacio CC, Spina CA, Richman DD. 1997. Recovery of replication-competent HIV despite prolonged suppression of plasma viremia. Science 278:1291–1295. https://doi.org/10.1126/science.278.5341.1291.

7. Hutter G, Nowak D, Mossner M, Ganepola S, Mussig A, Allers K, Schneider T, Hofmann J, Kucherer C, Blau O, Blau IW, Hofmann WK, Thiel E. 2009. Long-term control of HIV by CCR5 Δ32/Δ32 stem-cell transplantation. N Engl J Med 360:692–698. https://doi.org/10.1056/NEJMoa0802905.

8. Allers K, Hutter G, Hofmann J, Loddenkemper C, Rieger K, Thiel E, Schneider T. 2011. Evidence for the cure of HIV infection by CCR5Δ32/Δ32 stem cell transplantation. Blood 117:2791–2799. https://doi.org/10.1182/blood-2010-09-309591.

9. Gupta RK, Abdul-Jawad S, McCoy LE, Mok HP, Peppa D, Salgado M, Martinez-Picado J, Nijhuis M, Wensing AMJ, Lee H, Grant P, Nastouli E, Lambert J, Pace M, Salasc F, Monit C, Innes AJ, Muir L, Waters L, Frater J, Lever A, Edwards SG, Gabriel IH, Olavarria E. 2019. HIV-1 remission following CCR5Δ32/Δ32 haematopoietic stem-cell transplantation. Nature 568:244–248. https://doi.org/10.1038/s41586-019-1027-4.

10. Kim Y, Anderson JL, Lewin SR. 2018. Getting the "kill" into "shock and kill": strategies to eliminate latent HIV. Cell Host Microbe 23:14–26. https://doi.org/10.1016/j.chom.2017.12.004.

11. Bolton DL, Hahn BI, Park EA, Lehnhoff LL, Hornung F, Lenardo MJ. 2002. Death of CD4$^+$ T-cell lines caused by human immunodeficiency virus type 1 does not depend on caspases or apoptosis. J Virol 76:5094–5107. https://doi.org/10.1128/jvi.76.10.5094-5107.2002.

12. Shan L, Deng K, Shroff NS, Durand CM, Rabi SA, Yang HC, Zhang H, Margolick JB, Blankson JN, Siliciano RF. 2012. Stimulation of HIV-1-specific cytolytic T lymphocytes facilitates elimination of latent viral reservoir after virus reactivation. Immunity 36:491–501. https://doi.org/10.1016/j.immuni.2012.01.014.

13. Spivak AM, Planelles V. 2018. Novel latency reversal agents for HIV-1 cure. Annu Rev Med 69:421–436. https://doi.org/10.1146/annurev-med-052716-031710.

14. Ait-Ammar A, Kula A, Darcis G, Verdikt R, De Wit S, Gautier V, Mallon PWG, Marcello A, Rohr O, Van Lint C. 2019. Current status of latency reversing agents facing the heterogeneity of HIV-1 cellular and tissue reservoirs. Front Microbiol 10:3060–3060. https://doi.org/10.3389/fmicb.2019.03060.

15. Cillo AR, Sobolewski MD, Bosch RJ, Fyne E, Piatak M, Jr, Coffin JM, Mellors JW. 2014. Quantification of HIV-1 latency reversal in resting CD4$^+$ T cells from patients on suppressive antiretroviral therapy. Proc Natl Acad Sci U S A 111:7078–7083. https://doi.org/10.1073/pnas.1402873111.

16. Policicchio BB, Xu C, Brocca-Cofano E, Raehtz KD, He T, Ma D, Li H, Sivanandham R, Haret-Richter GS, Dunsmore T, Trichel A, Mellors JW, Hahn BH, Shaw GM, Ribeiro RM, Pandrea I, Apetrei C. 2016. Multi-dose romidepsin reactivates replication competent SIV in post-antiretroviral rhesus macaque controllers. PLoS Pathog 12:e1005879-e1005879. https://doi.org/10.1371/journal.ppat.1005879.

17. McBrien JB, Mavigner M, Franchitti L, Smith SA, White E, Tharp GK, Walum H, Busman-Sahay K, Aguilera-Sandoval CR, Thayer WO, Spagnuolo RA, Kovarova M, Wahl A, Cervasi B, Margolis DM, Vanderford TH, Carnathan DG, Paiardini M, Lifson JD, Lee JH, Safrit JT, Bosinger SE, Estes JD, Derdeyn CA, Garcia JV, Kulpa DA, Chahroudi A, Silvestri G. 2020. Robust and persistent reactivation of SIV and HIV by N-803 and depletion of CD8$^+$ cells. Nature 578:154–159. https://doi.org/10.1038/s41586-020-1946-0.

18. Richman DD, Margolis DM, Delaney M, Greene WC, Hazuda D, Pomerantz RJ. 2009. The challenge of finding a cure for HIV infection. Science 323:1304–1307. https://doi.org/10.1126/science.1165706.

19. Migueles SA, Weeks KA, Nou E, Berkley AM, Rood JE, Osborne CM, Hallahan CW, Cogliano-Shutta NA, Metcalf JA, McLaughlin M, Kwan R, Mican JM, Davey RT, Jr, Connors M. 2009. Defective human immunodeficiency virus-specific CD8$^+$ T-cell polyfunctionality, proliferation, and cytotoxicity are not restored by antiretroviral therapy. J Virol 83:11876–11889. https://doi.org/10.1128/JVI.01153-09.

20. Buckheit RW, III, Siliciano RF, Blankson JN. 2013. Primary CD8$^+$ T cells from elite suppressors effectively eliminate non-productively HIV-1 infected resting and activated CD4$^+$ T cells. Retrovirology 10:68. https://doi.org/10.1186/1742-4690-10-68.

21. Jones RB, O'Connor R, Mueller S, Foley M, Szeto GL, Karel D, Lichterfeld M, Kovacs C, Ostrowski MA, Trocha A, Irvine DJ, Walker BD. 2014. Histone deacetylase inhibitors impair the elimination of HIV-infected cells by cytotoxic T lymphocytes. PLoS Pathog 10:e1004287. https://doi.org/10.1371/journal.ppat.1004287.

22. Deng K, Pertea M, Rongvaux A, Wang L, Durand CM, Ghiaur G, Lai J, McHugh HL, Hao H, Zhang H, Margolick JB, Gurer C, Murphy AJ, Valenzuela DM, Yancopoulos GD, Deeks SG, Strowig T, Kumar P, Siliciano JD, Salzberg SL, Flavell RA, Shan L, Siliciano RF. 2015. Broad CTL response is required to clear latent HIV-1 due to dominance of escape mutations. Nature 517:381–385. https://doi.org/10.1038/nature14053.

23. Bruner KM, Murray AJ, Pollack RA, Soliman MG, Laskey SB, Capoferri AA, Lai J, Strain MC, Lada SM, Hoh R, Ho Y-C, Richman DD, Deeks SG, Siliciano JD, Siliciano RF. 2016. Defective proviruses rapidly accumulate during acute HIV-1 infection. Nat Med 22:1043–1049. https://doi.org/10.1038/nm.4156.

24. Mellors J. 2018. D-103 HIV cure: time to rethink the "shock and kill" strategy? AIDS 77:39. https://doi.org/10.1097/01.qai.0000532595.59554.19.

25. Battivelli E, Dahabieh MS, Abdel-Mohsen M, Svensson JP, Tojal Da Silva I, Cohn LB, Gramatica A, Deeks S, Greene WC, Pillai SK, Verdin E. 2018. Distinct chromatin functional states correlate with HIV latency reactivation in infected primary CD4$^+$ T cells. Elife 7:e34655. https://doi.org/10.7554/eLife.34655.

26. Shevach EM. 2011. Biological functions of regulatory T cells. Adv Immunol 112:137–176. https://doi.org/10.1016/B978-0-12-387827-4.00004-8.

27. He T, Brocca-Cofano E, Policicchio BB, Sivanandham R, Gautam R, Raehtz KD, Xu C, Pandrea I, Apetrei C. 2016. Cutting edge: T regulatory cell depletion reactivates latent simian immunodeficiency virus (SIV) in controller macaques while boosting SIV-specific T lymphocytes. J Immunol 197:4535–4539. https://doi.org/10.4049/jimmunol.1601539.

28. Schulze Zur Wiesch J, Thomssen A, Hartjen P, Toth I, Lehmann C, Meyer-Olson D, Colberg K, Frerk S, Babikir D, Schmiedel S, Degen O,

Mauss S, Rockstroh J, Staszewski S, Khaykin P, Strasak A, Lohse AW, Fatkenheuer G, Hauber J, van Lunzen J. 2011. Comprehensive analysis of frequency and phenotype of T regulatory cells in HIV infection: CD39 expression of FoxP3+ T regulatory cells correlates with progressive disease. J Virol 85:1287–1297. https://doi.org/10.1128/JVI.01758-10.

29. Presicce P, Orsborn K, King E, Pratt J, Fichtenbaum CJ, Chougnet CA. 2011. Frequency of circulating regulatory T cells increases during chronic HIV infection and is largely controlled by highly active antiretroviral therapy. PLoS One 6:e28118. https://doi.org/10.1371/journal .pone.0028118.

30. Andersson J, Boasso A, Nilsson J, Zhang R, Shire NJ, Lindback S, Shearer GM, Chougnet CA. 2005. Cutting edge: the prevalence of regulatory T cells in lymphoid tissue is correlated with viral load in HIV-infected patients. J Immunol 174:3143–3147. https://doi.org/10.4049/jimmunol .174.6.3143.

31. Nilsson J, Boasso A, Velilla PA, Zhang R, Vaccari M, Franchini G, Shearer GM, Andersson J, Chougnet C. 2006. HIV-1-driven regulatory T-cell accumulation in lymphoid tissues is associated with disease progression in HIV/AIDS. Blood 108:3808–3817. https://doi.org/10.1182/blood -2006-05-021576.

32. Suchard MS, Mayne E, Green VA, Shalekoff S, Donninger SL, Stevens WS, Gray CM, Tiemessen CT. 2010. FOXP3 expression is upregulated in CD4T cells in progressive HIV-1 infection and is a marker of disease severity. PLoS One 5:e11762-e11762. https://doi.org/10.1371/journal .pone.0011762.

33. Estes JD, Li Q, Reynolds MR, Wietgrefe S, Duan L, Schacker T, Picker LJ, Watkins DI, Lifson JD, Reilly C, Carlis J, Haase AT. 2006. Premature induction of an immunosuppressive regulatory T cell response during acute simian immunodeficiency virus infection. J Infect Dis 193: 703–712. https://doi.org/10.1086/500368.

34. Allers K, Loddenkemper C, Hofmann J, Unbehaun A, Kunkel D, Moos V, Kaup FJ, Stahl-Hennig C, Sauermann U, Epple HJ, Schneider T. 2010. Gut mucosal FOXP3+ regulatory CD4+ T cells and nonregulatory CD4+ T cells are differentially affected by simian immunodeficiency virus infection in rhesus macaques. J Virol 84:3259–3269. https://doi.org/10.1128/ JVI.01715-09.

35. Moreno-Fernandez ME, Zapata W, Blackard JT, Franchini G, Chougnet CA. 2009. Human regulatory T cells are targets for human immunodeficiency virus (HIV) infection, and their susceptibility differs depending on the HIV type 1 strain. J Virol 83:12925–12933. https://doi.org/10 .1128/JVI.01352-09.

36. Tran TA, de Goer de Herve MG, Hendel-Chavez H, Dembele B, Le Nevot E, Abbed K, Pallier C, Goujard C, Gasnault J, Delfraissy JF, Balazuc AM, Taoufik Y. 2008. Resting regulatory CD4 T cells: a site of HIV persistence in patients on long-term effective antiretroviral therapy. PLoS One 3:e3305. https://doi.org/10.1371/journal.pone.0003305.

37. Aandahl EM, Michaelsson J, Moretto WJ, Hecht FM, Nixon DF. 2004. Human CD4+ CD25+ regulatory T cells control T-cell responses to human immunodeficiency virus and cytomegalovirus antigens. J Virol 78:2454–2459. https://doi.org/10.1128/jvi.78.5.2454-2459.2004.

38. Carbonneil C, Donkova-Petrini V, Aouba A, Weiss L. 2004. Defective dendritic cell function in HIV-infected patients receiving effective highly active antiretroviral therapy: neutralization of IL-10 production and depletion of CD4+ CD25+ T cells restore high levels of HIV-specific CD4+ T cell responses induced by dendritic cells generated in the presence of IFN-α. J Immunol 172:7832–7840. https://doi.org/10.4049/ jimmunol.172.12.7832.

39. Kinter AL, Hennessey M, Bell A, Kern S, Lin Y, Daucher M, Planta M, McGlaughlin M, Jackson R, Ziegler SF, Fauci AS. 2004. CD25+ CD4+ regulatory T cells from the peripheral blood of asymptomatic HIV-infected individuals regulate CD4+ and CD8+ HIV-specific T cell immune responses in vitro and are associated with favorable clinical markers of disease status. J Exp Med 200:331–343. https://doi.org/10 .1084/jem.20032069.

40. Weiss L, Donkova-Petrini V, Caccavelli L, Balbo M, Carbonneil C, Levy Y. 2004. Human immunodeficiency virus-driven expansion of CD4+ CD25+ regulatory T cells, which suppress HIV-specific CD4 T-cell responses in HIV-infected patients. Blood 104:3249–3256. https://doi .org/10.1182/blood-2004-01-0365.

41. Bi X, Suzuki Y, Gatanaga H, Oka S. 2009. High frequency and proliferation of CD4+ FOXP3+ Treg in HIV-1-infected patients with low CD4 counts. Eur J Immunol 39:301–309. https://doi.org/10.1002/eji.200838667.

42. Nikolova M, Lelievre JD, Carriere M, Bensussan A, Levy Y. 2009. Regulatory T cells differentially modulate the maturation and apoptosis of

human CD8+ T-cell subsets. Blood 113:4556–4565. https://doi.org/10 .1182/blood-2008-04-151407.

43. Moreno-Fernandez ME, Presicce P, Chougnet CA. 2012. Homeostasis and function of regulatory T cells in HIV/SIV infection. J Virol 86: 10262–10269. https://doi.org/10.1128/JVI.00993-12.

44. Elahi S, Dinges WL, Lejarcegui N, Laing KJ, Collier AC, Koelle DM, McElrath MJ, Horton H. 2011. Protective HIV-specific CD8+ T cells evade Treg cell suppression. Nat Med 17:989–995. https://doi.org/10.1038/nm .2422.

45. Kleinman AJ, Sivanandham R, Pandrea I, Chougnet CA, Apetrei C. 2018. Regulatory T cells as potential targets for HIV cure research. Front Immunol 9:734–734. https://doi.org/10.3389/fimmu.2018.00734.

46. Khattri R, Cox T, Yasayko SA, Ramsdell F. 2003. An essential role for Scurfin in CD4+ CD25+ T regulatory cells. Nat Immunol 4:337–342. https://doi.org/10.1038/ni909.

47. Yagi H, Nomura T, Nakamura K, Yamazaki S, Kitawaki T, Hori S, Maeda M, Onodera M, Uchiyama T, Fujii S, Sakaguchi S. 2004. Crucial role of FOXP3 in the development and function of human CD25+ CD4+ regulatory T cells. Int Immunol 16:1643–1656. https://doi.org/10.1093/ intimm/dxh165.

48. Fontenot JD, Rasmussen JP, Gavin MA, Rudensky AY. 2005. A function for interleukin 2 in Foxp3-expressing regulatory T cells. Nat Immunol 6:1142–1151. https://doi.org/10.1038/ni1263.

49. Pandrea I, Gaufin T, Brenchley JM, Gautam R, Monjure C, Gautam A, Coleman C, Lackner AA, Ribeiro RM, Douek DC, Apetrei C. 2008. Cutting edge: experimentally induced immune activation in natural hosts of simian immunodeficiency virus induces significant increases in viral replication and CD4+ T cell depletion. J Immunol 181:6687–6691. https://doi.org/10.4049/jimmunol.181.10.6687.

50. Ni X, Jorgensen JL, Goswami M, Challagundla P, Decker WK, Kim YH, Duvic MA. 2015. Reduction of regulatory T cells by Mogamulizumab, a defucosylated anti-CC chemokine receptor 4 antibody, in patients with aggressive/refractory mycosis fungoides and Sezary syndrome. Clin Cancer Res 21:274–285. https://doi.org/10.1158/1078-0432.CCR-14-0830.

51. Selby MJ, Engelhardt JJ, Quigley M, Henning KA, Chen T, Srinivasan M, Korman AJ. 2013. Anti-CTLA-4 antibodies of IgG2a isotype enhance antitumor activity through reduction of intratumoral regulatory T cells. Cancer Immunol Res 1:32–42. https://doi.org/10.1158/2326-6066.CIR -13-0013.

52. Diao L, Hang Y, Othman AA, Mehta D, Amaravadi L, Nestorov I, Tran JQ. 2016. Population PK-PD analyses of CD25 occupancy, CD56bright NK cell expansion, and regulatory T cell reduction by daclizumab HYP in subjects with multiple sclerosis. Br J Clin Pharmacol 82:1333–1342. https://doi.org/10.1111/bcp.13051.

53. Nakamura K, Miki M, Mizoguchi Y, Karakawa S, Sato T, Kobayashi M. 2009. Deficiency of regulatory T cells in children with autoimmune neutropenia. Br J Haematol 145:642–647. https://doi.org/10.1111/j .1365-2141.2009.07662.x.

54. Kinnunen T, Chamberlain N, Morbach H, Choi J, Kim S, Craft J, Mayer L, Cancrini C, Passerini L, Bacchetta R, Ochs HD, Torgerson TR, Meffre E. 2013. Accumulation of peripheral autoreactive B cells in the absence of functional human regulatory T cells. Blood 121:1595–1603. https://doi .org/10.1182/blood-2012-09-457465.

55. Kim J, Lahl K, Hori S, Loddenkemper C, Chaudhry A, deRoos P, Rudensky A, Sparwasser T. 2009. Cutting edge: depletion of Foxp3+ cells leads to induction of autoimmunity by specific ablation of regulatory T cells in genetically targeted mice. J Immunol 183:7631–7634. https://doi.org/ 10.4049/jimmunol.0804308.

56. Ellis JS, Wan X, Braley-Mullen H. 2013. Transient depletion of CD4+ CD25+ regulatory T cells results in multiple autoimmune diseases in wild-type and B-cell-deficient NOD mice. Immunology 139:179–186. https://doi.org/10.1111/imm.12065.

57. Plitas G, Rudensky AY. 2016. Regulatory T cells: differentiation and function. Cancer Immunol Res 4:721–725. https://doi.org/10.1158/2326 -6066.CIR-16-0193.

58. Malek TR. 2008. The biology of interleukin-2. Annu Rev Immunol 26: 453–479. https://doi.org/10.1146/annurev.immunol.26.021607.090357.

59. Wang Z, Zheng Q, Zhang H, Bronson RT, Madsen JC, Sachs DH, Huang CA, Wang Z. 2017. Ontak-like human IL-2 fusion toxin. J Immunol Methods 448:51–58. https://doi.org/10.1016/j.jim.2017.05.008.

60. Yoshie O, Matsushima K. 2015. CCR4 and its ligands: from bench to bedside. Int Immunol 27:11–20. https://doi.org/10.1093/intimm/dxu079.

61. Ma D, Xu C, Cillo AR, Policicchio B, Kristoff J, Haret-Richter G, Mellors JW, Pandrea I, Apetrei C. 2015. Simian immunodeficiency virus SIVsab

infection of rhesus macaques as a model of complete immunological suppression with persistent reservoirs of replication-competent virus: implications for cure research. J Virol 89:6155–6160. https://doi.org/10.1128/JVI.00256-15.

62. Policicchio BB, Pandrea I, Apetrei C. 2016. Animal Models for HIV Cure Research. Front Immunol 7:12. https://doi.org/10.3389/fimmu.2016.00012.

63. Wang Z, Louras NJ, Lellouch AG, Pratts SG, Zhang H, Wang H, Huang CA, Cetrulo CL, Jr, Madsen JC, Sachs DH, Wang Z. 2018. Dosing optimization of CCR4 immunotoxin for improved depletion of CCR4+ Treg in nonhuman primates. Mol Oncol 12:1374–1382. https://doi.org/10.1002/1878-0261.12331.

64. Del Prete GQ, Smedley J, Macallister R, Jones GS, Li B, Hattersley J, Zheng J, Piatak M, Jr, Keele BF, Hesselgesser J, Geleziunas R, Lifson JD. 2016. Short communication: comparative evaluation of coformulated injectable combination antiretroviral therapy regimens in simian immunodeficiency virus-infected rhesus macaques. AIDS Res Hum Retroviruses 32:163–168. https://doi.org/10.1089/aid.2015.0130.

65. Deaglio S, Dwyer KM, Gao W, Friedman D, Usheva A, Erat A, Chen JF, Enjyoji K, Linden J, Oukka M, Kuchroo VK, Strom TB, Robson SC. 2007. Adenosine generation catalyzed by CD39 and CD73 expressed on regulatory T cells mediates immune suppression. J Exp Med 204:1257–1265. https://doi.org/10.1084/jem.20062512.

66. He T, Brocca-Cofano E, Gillespie DG, Xu C, Stock JL, Ma D, Policicchio BB, Raehtz KD, Rinaldo CR, Apetrei C, Jackson EK, Macatangay BJ, Pandrea I. 2015. Critical role for the adenosine pathway in controlling simian immunodeficiency virus-related immune activation and inflammation in gut mucosal tissues. J Virol 89:9616–9630. https://doi.org/10.1128/JVI.01196-15.

67. Avarbock AB, Loren AW, Park JY, Junkins-Hopkins JM, Choi J, Litzky LA, Rook AH. 2008. Lethal vascular leak syndrome after denileukin diftitox administration to a patient with cutaneous gamma/delta T-cell lymphoma and occult cirrhosis. Am J Hematol 83:593–595. https://doi.org/10.1002/ajh.21180.

68. Jeong GH, Lee KH, Lee IR, Oh JH, Kim DW, Shin JW, Kronbichler A, Eisenhut M, van der Vliet HJ, Abdel-Rahman O, Stubbs B, Solmi M, Veronese N, Dragioti E, Koyanagi A, Radua J, Shin JI. 2019. Incidence of capillary leak syndrome as an adverse effect of drugs in cancer patients: a systematic review and meta-analysis. J Clin Microbiol 8:143. https://doi.org/10.3390/jcm8020143.

69. Perna SK, De Angelis B, Pagliara D, Hasan ST, Zhang L, Mahendravada A, Heslop HE, Brenner MK, Rooney CM, Dotti G, Savoldo B. 2013. Interleukin 15 provides relief to CTLs from regulatory T cell-mediated inhibition: implications for adoptive T cell-based therapies for lymphoma. Clin Cancer Res 19:106–117. https://doi.org/10.1158/1078-0432.CCR-12-2143.

70. Akeus P, Szeponik L, Ahlmanner F, Sundström P, Alsén S, Gustavsson B, Sparwasser T, Raghavan S, Quiding-Järbrink M. 2018. Regulatory T cells control endothelial chemokine production and migration of T cells into intestinal tumors of APCmin/+ mice. Cancer Immunol Immunother 67:1067–1077. https://doi.org/10.1007/s00262-018-2161-9.

71. Hobbs TR, Blue SW, Park BS, Greisel JJ, Conn PM, Pau FKY. 2015. Measurement of blood volume in adult rhesus macaques (Macaca mulatta). J Am Assoc Lab Anim Sci 54:687–693.

72. Reilly C, Wietgrefe S, Sedgewick G, Haase A. 2007. Determination of simian immunodeficiency virus production by infected activated and resting cells. AIDS 21:163–168. https://doi.org/10.1097/QAD.0b013e328012565b.

73. Di Mascio M, Paik CH, Carrasquillo JA, Maeng J-S, Jang B-S, Shin IS, Srinivasula S, Byrum R, Neria A, Kopp W, Catalfamo M, Nishimura Y, Reimann K, Martin M, Lane HC. 2009. Noninvasive in vivo imaging of CD4 cells in simian-human immunodeficiency virus (SHIV)-infected nonhuman primates. Blood 114:328–337. https://doi.org/10.1182/blood-2008-12-192203.

74. Zhao H, Bo C, Kang Y, Li H. 2017. What else can CD39 tell us? Front Immunol 8:727. https://doi.org/10.3389/fimmu.2017.00727.

75. Borsellino G, Kleinewietfeld M, Di Mitri D, Sternjak A, Diamantini A, Giometto R, Hopner S, Centonze D, Bernardi G, Dell'Acqua ML, Rossini PM, Battistini L, Rotzschke O, Falk K. 2007. Expression of ectonucleotidase CD39 by Foxp3+ Treg cells: hydrolysis of extracellular ATP and immune suppression. Blood 110:1225–1232. https://doi.org/10.1182/blood-2006-12-064527.

76. Alam MS, Kurtz CC, Rowlett RM, Reuter BK, Wiznerowicz E, Das S, Linden J, Crowe SE, Ernst PB. 2009. CD73 is expressed by human regulatory T helper cells and suppresses proinflammatory cytokine production and Helicobacter felis-induced gastritis in mice. J Infect Dis 199:494–504. https://doi.org/10.1086/596205.

77. Sarhan D, Leijonhufvud C, Murray S, Witt K, Seitz C, Wallerius M, Xie H, Ullén A, Harmenberg U, Lidbrink E, Rolny C, Andersson J, Lundqvist A. 2017. Zoledronic acid inhibits NFAT and IL-2 signaling pathways in regulatory T cells and diminishes their suppressive function in patients with metastatic cancer. Oncoimmunology 6:e1338238. https://doi.org/10.1080/2162402X.2017.1338238.

78. Cecchinato V, Tryniszewska E, Ma ZM, Vaccari M, Boasso A, Tsai WP, Petrovas C, Fuchs D, Heraud JM, Venzon D, Shearer GM, Koup RA, Lowy I, Miller CJ, Franchini G. 2008. Immune activation driven by CTLA-4 blockade augments viral replication at mucosal sites in simian immunodeficiency virus infection. J Immunol 180:5439–5447. https://doi.org/10.4049/jimmunol.180.8.5439.

79. Hryniewicz A, Boasso A, Edghill-Smith Y, Vaccari M, Fuchs D, Venzon D, Nacsa J, Betts MR, Tsai W-P, Heraud J-M, Beer B, Blanset D, Chougnet C, Lowy I, Shearer GM, Franchini G. 2006. CTLA-4 blockade decreases TGF-β, IDO, and viral RNA expression in tissues of SIVmac251-infected macaques. Blood 108:3834–3842. https://doi.org/10.1182/blood-2006-04-010637.

80. Pandrea I, Apetrei C, Dufour J, Dillon N, Barbercheck J, Metzger M, Jacquelin B, Bohm R, Marx PA, Barre-Sinoussi F, Hirsch VM, Muller-Trutwin MC, Lackner AA, Veazey RS. 2006. Simian immunodeficiency virus SIVagm.sab infection of Caribbean African green monkeys: a new model for the study of SIV pathogenesis in natural hosts. J Virol 80:4858–4867. https://doi.org/10.1128/JVI.80.10.4858-4867.2006.

81. Pandrea I, Kornfeld C, Ploquin MJ-Y, Apetrei C, Faye A, Rouquet P, Roques P, Simon F, Barré-Sinoussi F, Müller-Trutwin MC, Diop OM. 2005. Impact of viral factors on very early in vivo replication profiles in simian immunodeficiency virus SIVagm-infected African green monkeys. J Virol 79:6249–6259. https://doi.org/10.1128/JVI.79.10.6249-6259.2005.

82. Pandrea I, Gaufin T, Gautam R, Kristoff J, Mandell D, Montefiori D, Keele BF, Ribeiro RM, Veazey RS, Apetrei C. 2011. Functional cure of SIVagm infection in rhesus macaques results in complete recovery of CD4+ T cells and is reverted by CD8+ cell depletion. PLoS Pathog 7:e1002170. https://doi.org/10.1371/journal.ppat.1002170.

83. National Research Council. 1996. Guide for the care and use of laboratory animals. National Academy Press, Washington, DC.

84. Peraino JS, Zhang H, Rajasekera PV, Wei M, Madsen JC, Sachs DH, Huang CA, Wang Z. 2014. Diphtheria toxin-based bivalent human IL-2 fusion toxin with improved efficacy for targeting human CD25+ cells. J Immunol Methods 405:57–66. https://doi.org/10.1016/j.jim.2014.01.008.

85. Sugiyama D, Nishikawa H, Maeda Y, Nishioka M, Tanemura A, Katayama I, Ezoe S, Kanakura Y, Sato E, Fukumori Y, Karbach J, Jäger E, Sakaguchi S. 2013. Anti-CCR4 MAb selectively depletes effector-type FoxP3+ CD4+ regulatory T cells, evoking antitumor immune responses in humans. Proc Natl Acad Sci U S A 110:17945–17950. https://doi.org/10.1073/pnas.1316791110.

86. Wang Z, Navarro-Alvarez N, Shah JA, Zhang H, Huang Q, Zheng Q, Madsen JC, Sachs DH, Huang CA, Wang Z. 2016. Porcine Treg depletion with a novel diphtheria toxin-based anti-human CCR4 immunotoxin. Vet Immunol Immunopathol 182:150–158. https://doi.org/10.1016/j.vetimm.2016.10.014.

87. Wang Z, Pratts SG, Zhang H, Spencer PJ, Yu R, Tonsho M, Shah JA, Tanabe T, Powell HR, Huang CA, Madsen JC, Sachs DH, Wang Z. 2016. Treg depletion in non-human primates using a novel diphtheria toxin-based anti-human CCR4 immunotoxin. Mol Oncol 10:553–565. https://doi.org/10.1016/j.molonc.2015.11.008.

88. Wang Z, Wei M, Zhang H, Chen H, Germana S, Huang CA, Madsen JC, Sachs DH, Wang Z. 2015. Diphtheria-toxin based anti-human CCR4 immunotoxin for targeting human CCR4+ cells in vivo. Mol Oncol 9:1458–1470. https://doi.org/10.1016/j.molonc.2015.04.004.

89. Kaminetzky D, Hymes KB. 2008. Denileukin diftitox for the treatment of cutaneous T-cell lymphoma. Biologics 2:717–724. https://doi.org/10.2147/btt.s3084.

90. Atchison E, Eklund J, Martone B, Wang L, Gidron A, Macvicar G, Rademaker A, Goolsby C, Marszalek L, Kozlowski J, Smith N, Kuzel TM. 2010. A pilot study of denileukin diftitox (DD) in combination with high-dose interleukin-2 (IL-2) for patients with metastatic renal cell carcinoma (RCC). J Immunother 33:716–722. https://doi.org/10.1097/CJI.0b013e3181e4752e.

91. Foss FM, Sjak-Shie N, Goy A, Jacobsen E, Advani R, Smith MR, Komrokji R, Pendergrass K, Bolejack V. 2013. A multicenter phase II trial to determine the safety and efficacy of combination therapy with denileukin diftitox and cyclophosphamide, doxorubicin, vincristine and prednisone in untreated peripheral T-cell lymphoma: the CONCEPT study. Leuk Lymphoma 54:1373–1379. https://doi.org/10.3109/10428194.2012.742521.

92. Telang S, Rasku MA, Clem AL, Carter K, Klarer AC, Badger WR, Milam RA, Rai SN, Pan J, Gragg H, Clem BF, McMasters KM, Miller DM, Chesney J. 2011. Phase II trial of the regulatory T cell-depleting agent, denileukin diftitox, in patients with unresectable stage IV melanoma. BMC Cancer 11:515. https://doi.org/10.1186/1471-2407-11-515.

93. Pandrea I, Ribeiro RM, Gautam R, Gaufin T, Pattison M, Barnes M, Monjure C, Stoulig C, Dufour J, Cyprian W, Silvestri G, Miller MD, Perelson AS, Apetrei C. 2008. Simian immunodeficiency virus SIVagm dynamics in African green monkeys. J Virol 82:3713–3724. https://doi.org/10.1128/JVI.02402-07.

94. Brocca-Cofano E, Xu C, Wetzel KS, Cottrell ML, Policicchio BB, Raehtz KD, Ma D, Dunsmore T, Haret-Richter GS, Musaitif K, Keele BF, Kashuba AD, Collman RG, Pandrea I, Apetrei C. 2018. Marginal effects of systemic CCR5 blockade with maraviroc on oral simian immunodeficiency virus transmission to infant macaques. J Virol 92:e00576-18. https://doi.org/10.1128/JVI.00576-18.

95. Pandrea I, Silvestri G, Onanga R, Veazey RS, Marx PA, Hirsch V, Apetrei C. 2006. Simian immunodeficiency viruses replication dynamics in African non-human primate hosts: common patterns and species-specific differences. J Med Primatol 35:194–201. https://doi.org/10.1111/j.1600-0684.2006.00168.x.

96. He T, Xu C, Krampe N, Dillon SM, Sette P, Falwell E, Haret-Richter GS, Butterfield T, Dunsmore TL, McFadden WM, Jr, Martin KJ, Policicchio BB, Raehtz KD, Penn EP, Tracy RP, Ribeiro RM, Frank DN, Wilson CC, Landay AL, Apetrei C, Pandrea I. 2019. High-fat diet exacerbates SIV pathogen-esis and accelerates disease progression. J Clin Invest 129:5474–5488. https://doi.org/10.1172/JCI121208.

97. Pandrea I, Xu C, Stock JL, Frank DN, Ma D, Policicchio BB, He T, Kristoff J, Cornell E, Haret-Richter GS, Trichel A, Ribeiro RM, Tracy R, Wilson C, Landay AL, Apetrei C. 2016. Antibiotic and antiinflammatory therapy transiently reduces inflammation and hypercoagulation in acutely SIV-infected pigtailed macaques. PLoS Pathog 12:e1005384. https://doi.org/10.1371/journal.ppat.1005384.

98. Gautam R, Gaufin T, Butler I, Gautam A, Barnes M, Mandell D, Pattison M, Tatum C, Macfarland J, Monjure C, Marx PA, Pandrea I, Apetrei C. 2009. Simian immunodeficiency virus SIVrcm, a unique CCR2-tropic virus, selectively depletes memory CD4$^+$ T cells in pigtailed macaques through expanded coreceptor usage in vivo. J Virol 83:7894–7908. https://doi.org/10.1128/JVI.00444-09.

99. Ma D, Jasinska A, Kristoff J, Grobler JP, Turner T, Jung Y, Schmitt C, Raehtz K, Feyertag F, Martinez Sosa N, Wijewardana V, Burke DS, Robertson DL, Tracy R, Pandrea I, Freimer N, Apetrei C, International Vervet Research C. 2013. SIVagm infection in wild African green monkeys from South Africa: epidemiology, natural history, and evolutionary considerations. PLoS Pathog 9:e1003011. https://doi.org/10.1371/journal.ppat.1003011.

100. Gaufin T, Pattison M, Gautam R, Stoulig C, Dufour J, MacFarland J, Mandell D, Tatum C, Marx MH, Ribeiro RM, Montefiori D, Apetrei C, Pandrea I. 2009. Effect of B-cell depletion on viral replication and clinical outcome of simian immunodeficiency virus infection in a natural host. J Virol 83:10347–10357. https://doi.org/10.1128/JVI.00880-09.